2012-12

Three-dimensional structure of thermohaline staircases in the tropical north Atlantic and their effect on acoustic propagation

Bulters, Amy C.

Monterey, California. Naval Postgraduate School

NAVAL POSTGRADUATE SCHOOL

MONTEREY, CALIFORNIA

THESIS

THREE-DIMENSIONAL STRUCTURE OF THERMOHALINE STAIRCASES IN THE TROPICAL NORTH ATLANTIC AND THEIR EFFECT ON ACOUSTIC PROPAGATION

by

Amy C. Bulters

December 2012

Thesis Advisor: Timour Radko
Second Reader: John Joseph

Approved for public release; distribution is unlimited

THIS PAGE INTENTIONALLY LEFT BLANK

REPORT DOCUMENTATION PAGE	Form Approved OMB No. 0704-0188

1. AGENCY USE ONLY *(Leave blank)*	2. REPORT DATE December 2012	3. REPORT TYPE AND DATES COVERED Master's Thesis

4. TITLE AND SUBTITLE THREE-DIMENSIONAL STRUCTURE OF THERMOHALINE STAIRCASES IN THE TROPICAL NORTH ATLANTIC AND THEIR EFFECT ON ACOUSTIC PROPAGATION	5. FUNDING NUMBERS
6. AUTHOR(S) Amy C. Bulters	
7. PERFORMING ORGANIZATION NAME(S) AND ADDRESS(ES) Naval Postgraduate School Monterey, CA 93943-5000	8. PERFORMING ORGANIZATION REPORT NUMBER
9. SPONSORING /MONITORING AGENCY NAME(S) AND ADDRESS(ES) N/A	10. SPONSORING/MONITORING AGENCY REPORT NUMBER

11. SUPPLEMENTARY NOTES The views expressed in this thesis are those of the author and do not reflect the official policy or position of the Department of Defense or the U.S. Government. IRB Protocol number ____N/A____.

12a. DISTRIBUTION / AVAILABILITY STATEMENT Approved for public release; distribution is unlimited	12b. DISTRIBUTION CODE

Under typical conditions in the subtropical thermocline double-diffusion occurs in the form of salt fingering (warm, salty fluid overlies cold, fresh fluid). The formation of staircases in the thermohaline structure of the ocean has been observed since the late 1960s, with recent field data collected within the tropical Atlantic displaying staircases with high-gradient interfaces characterized by a unique spatial orientation determined by background temperature and salinity. Competing theories have been proposed to explain the dynamics of these staircases; however, the origin of the staircases and the mechanism that controls final equilibrium remains poorly understood. This thesis examines staircase development in the tropical Atlantic. Incorporating double diffusion using the flux-gradient formulation of Radko and Smith, staircases are numerically simulated to resolve the controversial aspects of the staircase theories. The staircase simulations are critically evaluated against the C-SALT experiment observations, and the conditions for their formation and explanation of the fully equilibrated state are resolved and explained. The effect of acoustic propagation through the three-dimensional modeled staircases is evaluated to determine the impact of these large staircase areas on various frequencies and depths.

14. SUBJECT TERMS Double Diffusion, Salt Fingers, Thermohaline staircase, Acoustic propagation, C-SALT, Density Ratio	15. NUMBER OF PAGES 93
	16. PRICE CODE

17. SECURITY CLASSIFICATION OF REPORT	18. SECURITY CLASSIFICATION OF THIS PAGE	19. SECURITY CLASSIFICATION OF ABSTRACT	20. LIMITATION OF ABSTRACT
Unclassified	Unclassified	Unclassified	UU

NSN 7540-01-280-5500 Standard Form 298 (Rev. 2-89)
Prescribed by ANSI Std. 239-18

THIS PAGE INTENTIONALLY LEFT BLANK

Approved for public release; distribution is unlimited

THREE-DIMENSIONAL STRUCTURE OF THERMOHALINE STAIRCASES IN THE TROPICAL NORTH ATLANTIC AND THEIR EFFECT ON ACOUSTIC PROPAGATION

Amy C. Bulters
Lieutenant, Royal Australian Navy
B.S., University of New South Wales (ADFA), 2001
Grad.Dip.Met, Bureau of Meteorology, 2007

Submitted in partial fulfillment of the
requirements for the degree of

MASTER OF SCIENCE IN PHYSICAL OCEANOGRAPHY

from the

NAVAL POSTGRADUATE SCHOOL
December 2012

Author: Amy C. Bulters

Approved by: Timour Radko
Thesis Advisor

John Joseph
Second Reader

Peter Chu
Chair, Department of Oceanography

THIS PAGE INTENTIONALLY LEFT BLANK

ABSTRACT

Under typical conditions in the subtropical thermocline double-diffusion occurs in the form of salt fingering (warm, salty fluid overlies cold, fresh fluid). The formation of staircases in the thermohaline structure of the ocean has been observed since the late 1960s, with recent field data collected within the tropical Atlantic displaying staircases with high-gradient interfaces characterized by a unique spatial orientation determined by background temperature and salinity. Competing theories have been proposed to explain the dynamics of these staircases; however, the origin of the staircases and the mechanism that controls final equilibrium remains poorly understood. This thesis examines staircase development in the tropical Atlantic. Incorporating double diffusion using the flux-gradient formulation of Radko and Smith, staircases are numerically simulated to resolve the controversial aspects of the staircase theories. The staircase simulations are critically evaluated against the C-SALT experiment observations, and the conditions for their formation and explanation of the fully equilibrated state are resolved and explained. The effect of acoustic propagation through the three-dimensional modeled staircases is evaluated to determine the impact of these large staircase areas on various frequencies and depths.

THIS PAGE INTENTIONALLY LEFT BLANK

TABLE OF CONTENTS

I. INTRODUCTION 1
A. DOUBLE DIFFUSION 1
1. History 1
2. Salt Fingers 2
3. Thermohaline Staircases 3
4. Theoretical Background 4
B. C-SALT 5

II. LATERAL COHERENCE, MERGING, AND ALIGNMENT OF THERMOHALINE STAIRCASES 7
A. LATERAL COHERENCE 7
1. C-SALT Observations 7
B. MERGING 10
1. Theory 10
C. ALIGNMENT WITH BACKGROUND FLOW 11

III. SIMULATION OF STAIRCASES–EVOLUTION AND ALIGNMENT 15
A. MODEL SETUP 15
1. Massachusetts Institute of Technology General Circulation Model (MITgcm) 15
2. Initial Datasets 16
3. Model runs performed without Double Diffusion and with Constant Flux Ratio 18
B. MODEL RESULTS 21
1. Effects of Vertical Eddy Diffusivities 21
2. Mechanism of Merging and Growth Rates 25
3. Lateral Coherence of Modeled Layers 31
4. Alignment of Interface Slopes with Background Flow 34

IV. STAIRCASE EFFECTS ON ACOUSTIC PROPOGATION 37
A. BACKGROUND 37
B. PROCESS 38
C. RESULTS 43
1. Source Depth 5 m 43
a. Ray Trace 43
b. Transmission Loss 44
2. Source Depth 387 m 46
a. Ray Trace 46
b. Transmission Loss 48
3. Source Depth 450 m 51
a. Ray Trace 51
b. Transmission Loss 53
4. Range-Dependent Source in Layer 57

a. Ray Trace *57*
b. Transmission Loss *59*
5. Range-Dependent Source in Interface 62
a. Ray Trace *62*
b. Transmission Loss *63*
V. CONCLUSIONS 67
LIST OF REFERENCES 69
INITIAL DISTRIBUTION LIST 73

LIST OF FIGURES

Figure 1. Schematic diagram illustrating the physical mechanisms of salt fingering (From Ruddick and Kerr, 2003) 3

Figure 2. Area of C-SALT survey (From Schmitt, 1987) 6

Figure 3. Three-dimensional view of CTD tow-yo (rear profile to the south) as the ship steamed to the north. 1.3 km separation between profiles, 33 km total distance covered (From Schmitt et al. 1987). 7

Figure 4. XBT temperature profiles from east to west, with 5.5 km separation between drops and total distance of 220 km. The profile at far left is correct, each subsequent profile is offset by 1.6 °c (From Schmitt 1987). 8

Figure 5. Potential temperature—salinity values of layers from CTD stations during C-SALT. Solid circles are from layers greater than 10 m thick, open circles are from layers 5–10 m thick. Hashed lines are temperature-salinity relationship obtained from stations at northwest and southeast corners of the survey. Solid lines represent isopycnal surfaces (From Schmitt 1987). 9

Figure 6. Basic two layer interface (from Wall 2007) 12

Figure 7. Temperature and Salinity at the surface and at 1000m depth, and Density Ratio, at initialization. 17

Figure 8. Vertical Temperature profile with constant flux ratio, $\gamma = 0.5128$. 19

Figure 9. Vertical Temperature profile with the effects of double diffusion removed from the model. 20

Figure 10. Vertical Temperature profile with flux ratio from Equation 10 and active double diffusion. .. 20

Figure 11. Total flux ratio versus density ratio (left) and density ratio (right) for $K_T = T_S = 0 \quad m^2/s$. Upon analysis staircases are evident throughout the region. 23

Figure 12. Total flux ratio versus density ratio (left) and density ratio (right) for $K_T = K_S = 10^{-6} \quad m^2/s$.

Staircases are largely prevalent throughout the region as indicated by contours. 23
Figure 13. Total flux ratio versus density ratio (left) and density ratio (right) for $K_T = K_S = 2.5*10^{-6}$ m^2/s. Staircases are evident a region similar to that observed in the C-SALT experiment. 24
Figure 14. Total flux ratio versus density ratio (left) and density ratio (right) for $K_T = K_S = 10^{-5}$ m^2/s. Staircases are almost completely absent at this vertical eddy diffusivity. 24
Figure 15. Three-dimensional visualization at t=0 secs. 25
Figure 16. Three-dimensional visualization at t=10 years. Staircases are evident at this time and layers have commenced growth through merging. 26
Figure 17. Three-dimensional visualization at t=18.6 years with evident staircases merged to equilibrium. 26
Figure 18. Formation and evolution of layers in the numerical model shown at (a-d) t=0, 5.4 , 9.2, 10.4 years. 27
Figure 19. Evolution of layers in the numerical model shown at (a-d) t=14.7, 15.9, 17.7, 18.6 years. . 28
Figure 20. Space-time diagram of the numerically modeled temperature gradient ($^{\circ}c/m$). Layers merge when the relatively strong interfaces grow further at the expense of weaker interfaces, which decay and eventually disappear (B-merger scenario). 29
Figure 21. Change in temperature vs. time during merging event 1. 30
Figure 22. Change in temperature vs. time during merging event 2. 30
Figure 23. Temperature-salinity values taken from three individual layers in the model. Each color represents a separate layer. 32
Figure 24. Series of offset temperature profiles from the DNS in an east to west section with 10 km separation. The right-most profile lies to the east of the others; the total distance covered is 290km. The temperature scale is correct for the left-most profile and each subsequent profile is offset 1.6 $^{\circ}C$ 33

Figure 25. Temperature profiles from Figure 24, focused at the depth of staircase formation. 33
Figure 26. C-SALT Station 20 Temperature profile (left) with upper 1000m displayed (right). 40
Figure 27. C-SALT Station 20 SSP (left) with upper 1000 m displayed (right). 41
Figure 28. C-SALT Station 20 SSP (left) and smoothed profile (right). 42
Figure 29. C-SALT Station 20 SSP to depth 700 m (left) and smoothed SSP to depth 700 m (right) 42
Figure 30. Ray Trace profile for a source at 5 m in a staircase environment. The ray trace is nearly identical to that which occurs for a smoothed profile. 44
Figure 31. Coherent transmission loss (dB/m) for a source at 5 m depth and 2000 Hz frequency for a smoothed environment. 45
Figure 32. Coherent transmission loss (dB/m) for a source at 5 m depth and 2000 Hz frequency for a stepped environment. 46
Figure 33. Ray Trace for source at 387 m (depth of an interface) in a staircase environment. 47
Figure 34. Ray trace for a source at 387 m in a smoothed profile. 47
Figure 35. Coherent TL (dB/m) for stepped profile with source in interface at 50 Hz 48
Figure 36. Coherent TL (dB/m) for smooth profile with 50 Hz source at 387 m. 49
Figure 37. Coherent TL (dB/m) for stepped profile with source in interface at 2000 Hz. 49
Figure 38. Coherent TL (dB/m) for smooth profile with 2000 Hz source at 387 m. 50
Figure 39. Coherent TL (dB/m) for stepped environment with source in interface at 5000 Hz. 50
Figure 40. Coherent TL (dB/m) for 5000 Hz source in smooth profile at 387 m. 51
Figure 41. Ray trace with source at 450 m (center of vertically mixed layer) in a staircase environment. 52
Figure 42. Ray trace with source depth 450 m in a smoothed profile. 52

Figure 43. Coherent TL (dB/m) for stepped profile with 50 Hz source in layer. 54
Figure 44. Coherent TL (dB/m) for 50Hz source at 450m in a smoothed environment. 54
Figure 45. Coherent TL (dB/m) for stepped profile with 2000 Hz source in layer. 55
Figure 46. Coherent TL (dB/m) for 2000 Hz source at 450m in smoothed profile. 55
Figure 47. Coherent TL (dB/m) for 5000 Hz source in layer of stepped profile. 56
Figure 48. Coherent TL (dB/m) for 5000 Hz source at 450 m in smoothed profile. 56
Figure 49. Ray trace for source at 785 m (source in layer), in a range dependent staircase environment. 58
Figure 50. Range-dependent sound speed profiles at 10 km spacing. 58
Figure 51. Sound speed (m/s) as a function of depth and range due to laterally coherent staircases. 59
Figure 52. Coherent TL (dB/m) for 50 Hz source within layer. 60
Figure 53. Coherent TL (dB/m) for 500 Hz within layer. 61
Figure 54. Coherent TL (dB/m) for 2000 Hz within layer. 61
Figure 55. Coherent TL (dB/m) for 5000 Hz within a layer. .. 62
Figure 56. Ray trace for source at staircase interface for range-dependent profiles. 63
Figure 57. Coherent TL (dB/m) for 50 Hz source at interface. 64
Figure 58. Coherent TL (dB/m) for 500 Hz source at interface. 64
Figure 59. Coherent TL (dB/m) for 2000 Hz source at interface. 65
Figure 60. Coherent TL (dB/m) for 5000 Hz source at interface depth. 65

LIST OF TABLES

Table 1. Parameter values in the numerical model. 22

THIS PAGE INTENTIONALLY LEFT BLANK

LIST OF ACRONYMS AND ABBREVIATIONS

ERDC	Engineering Research and Development Centre
C-SALT	Caribbean Sheets and Layers Transect
XBT	Bathythermograph
DNS	Direct Numerical Simulation
MITgcm	Massachusetts Institute of Technology General Circulation Model
DoD	Department of Defense
HPCMP Program	High Performance Computing Modernization
NODC_WOA98	National Oceanographic Data Centre World Ocean Atlas 1998
KPP	K Profile parameterization
PE	Parabolic Equation
SSP	Sound Speed Profile
TL	Transmission Loss

THIS PAGE INTENTIONALLY LEFT BLANK

ACKNOWLEDGMENTS

First and foremost, I would like to thank my advisor, Dr. Timour Radko, for his guidance, patience and dedication in this project. Even in the darkest and most frustrating hours of data processing and simulating, his unwavering enthusiasm, bright temperament and professional encouragement is the only reason this project progressed. His knowledge on this subject cannot be overstated and I feel privileged to have been afforded the opportunity to work with a pioneer in the field.

I would also like to thank Dr. Jason Flanagan. His expertise on all things MATLAB, MITgcm, and Linux, along with his willingness to share this knowledge and his valuable time with me, was greatly appreciated. I would like to thank John Joseph for his assistance and guidance, which allowed me to direct this thesis into an area of tactical significance to the Navy. Thanks must also go to Mike Cook for his assistance with MATLAB, and to Dr. Jean-Michel Campin, who was always more than willing to field my phone calls and provide guidance on MITgcm questions.

Thanks to my many friends and colleagues who took me in and made me feel as though I was at home while studying abroad, and particular thanks must go to Angela and Erlina, who provided a sounding board for my thoughts on many occasions.

This work was supported in part by a grant of computer time from the DoD High Performance Computing Modernization Program at the Engineering Research and Development Centre (ERDC).

THIS PAGE INTENTIONALLY LEFT BLANK

I. INTRODUCTION

A. DOUBLE DIFFUSION

1. History

Double diffusion is a phenomenon that occurs due to the differing molecular diffusivities of two properties (e.g.; temperature and salinity), within a stably stratified fluid. Double-diffusion operates in configurations in which these properties have an opposing effect on the stability of the water column.

Double diffusion is a relatively recent discovery in the realm of science (Stern 1960), although W. Stanley Jevons, an English economist, came very close to discovering it in 1857 when he created sugar fingers during an experiment. Although Jevons understood that heat diffused faster than the dissolved sugar, his statement that "all convection should occur as minute streamlets" failed to capture the physics behind the phenomenon (Schmitt 1995).

Whilst others would go on to attempt to explain the phenomena, including the English physicist Lord Rayleigh, the subject was correctly explained only in the mid-20th century by Melvin Stern (1960). Stern's discovery was motivated by an experiment by his colleagues, Stommel, Arons and Blanchard (1956), who developed the Perpetual Salt Fountain. This was an experiment initially designed to test pressure at the base of an ocean, by inserting a narrow heat-conducting pipe vertically to draw water to the surface. Due to the lower salinity of the basal water, once at thermal equilibrium it would continue to rise towards

the surface due to being lighter than its surrounds. While investigating this idea, the concept that placing a spigot on the top of the tube would cause the water to run continuously was introduced, thus the "Perpetual Salt Fountain" was born. Stern took this experiment to the next step, realizing that salt fountains occur naturally in the ocean, as a result of heat conducting 100 times faster than the diffusion of salt in the ocean. Hence thermal equilibrium of a parcel of water with its surroundings can occur faster than chemical equilibrium, resulting in an ocean containing parcels with differing salinities adjacent to each other devoid of a salt fountain pipe. Different salinities result in different density gradients, and thus motion dubbed as double diffusive convection.

2. Salt Fingers

There are two types of double diffusive convection in the ocean. The first is when cold, fresh water overlies salty, warm water. If a warm salty parcel is displaced upward, due to the difference in molecular diffusivity it cools much quicker then it loses salinity, thus becoming denser than its surroundings and sinking back down. As it sinks it regains heat quickly, but is now less saline than its surroundings, thus rising again, this time further than it did previously. This process can continue to occur, slowly mixing the water column. This is known as diffusive convection. The other type is salt fingering, which occurs when warm, salty water overlies cold, fresh water. If the warm, salty parcel is displaced downward, as in the previous example it will lose heat quicker than salinity, becoming denser than its surroundings, and thus continuing

to sink. These parcels appear as thin elongated streams, only 1 to 5 centimeters wide, and tens of centimeters long.

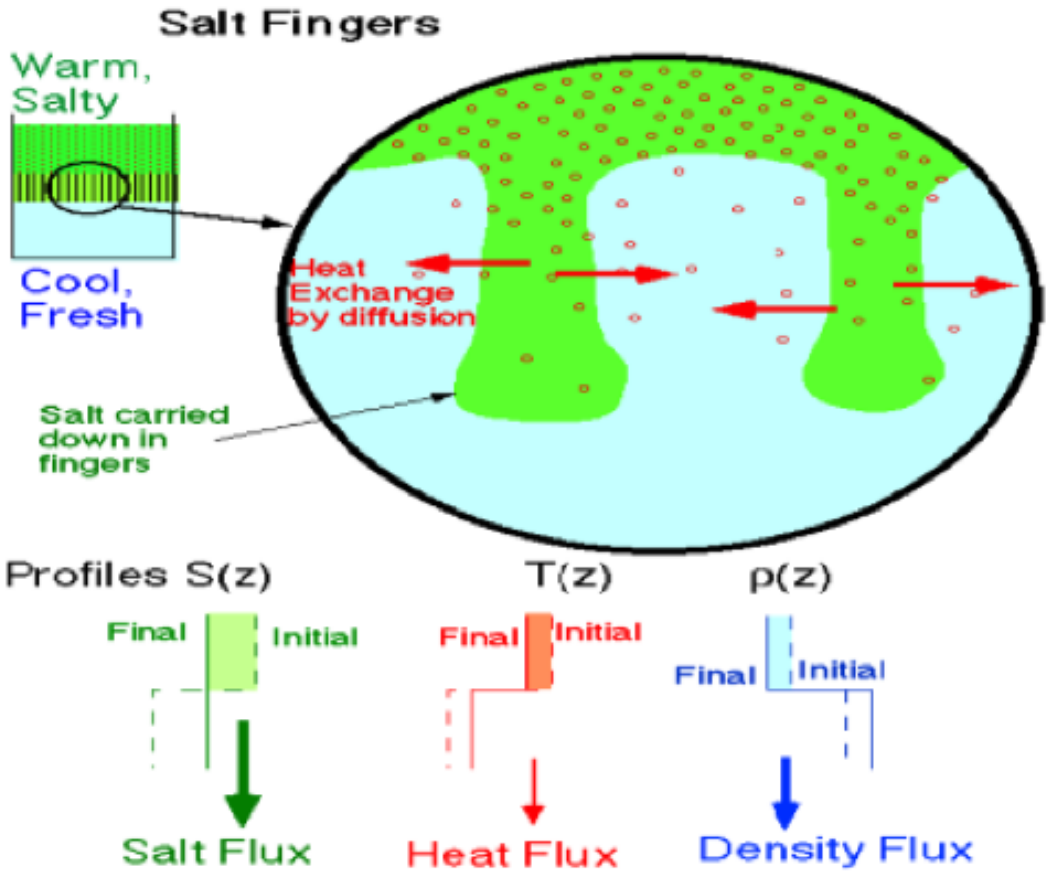

Figure 1. Schematic diagram illustrating the physical mechanisms of salt fingering (From Ruddick and Kerr, 2003)

3. Thermohaline Staircases

In the ocean, vertical stratification is often characterized by the appearance of well-mixed layers separated by fine interfaces with large temperature and salinity gradients, known as thermohaline staircases. The interfaces of these staircases are occupied by salt fingers, which cause a net unstable buoyancy flux that

stirs the layers (Stern and Turner 1969). This stirring of the layers can result in vertical growth of the layer through destruction of the interface and merging of the layers.

There is a large abundance of these staircase regions throughout the world, and the increased temperature and salinity fluxes in these staircases (Schmitt 2005) suggest that they play an important role in global ocean mixing.

4. Theoretical Background

The density ratio controls the intensity of salt fingering and is defined by:

$$R_\rho = \frac{\alpha \Delta T}{\beta \Delta S} \tag{1}$$

where, α is the thermal expansion coefficient and β is the saline expansion coefficient. If the density ratio is less than one, then the density gradient is unstable and will overturn. High values of density ratio correspond to weak double diffusive mixing, whereas density ratios that are slightly above unity are associated with vigorous fingering.

Another important parameter in the formation of salt fingers is the flux ratio,

$$\gamma = \frac{\alpha F_T}{\beta F_S} \tag{2}$$

where F_T and F_S are the molecular fluxes of heat and salt, respectively. This value must theoretically be below one to satisfy the net transport of density "up gradient."

B. C-SALT

In 1985, a field program by the name of Caribbean-Sheets and Layer Transects (C-SALT) was carried out in the tropical North Atlantic Ocean east of Barbados to survey the thermohaline staircases in the area, developed due to vertical mixing by salt fingers. The survey area lies between 150m and 750m depth, at the confluence of the highly saline Subtropical Underwater and the fresher Antarctic Intermediate water, and this gives rise to a very strong destabilizing salinity gradient which can drive salt fingers (Schmitt 1987). The temperature profiles in the survey were classified as layered, weakly layered or nonlayered, with an area within 10° and 14°N, and 52° and 57°W having the thickest mixed layers, largest number of layers, and largest temperature differences, as seen in Figure 2.

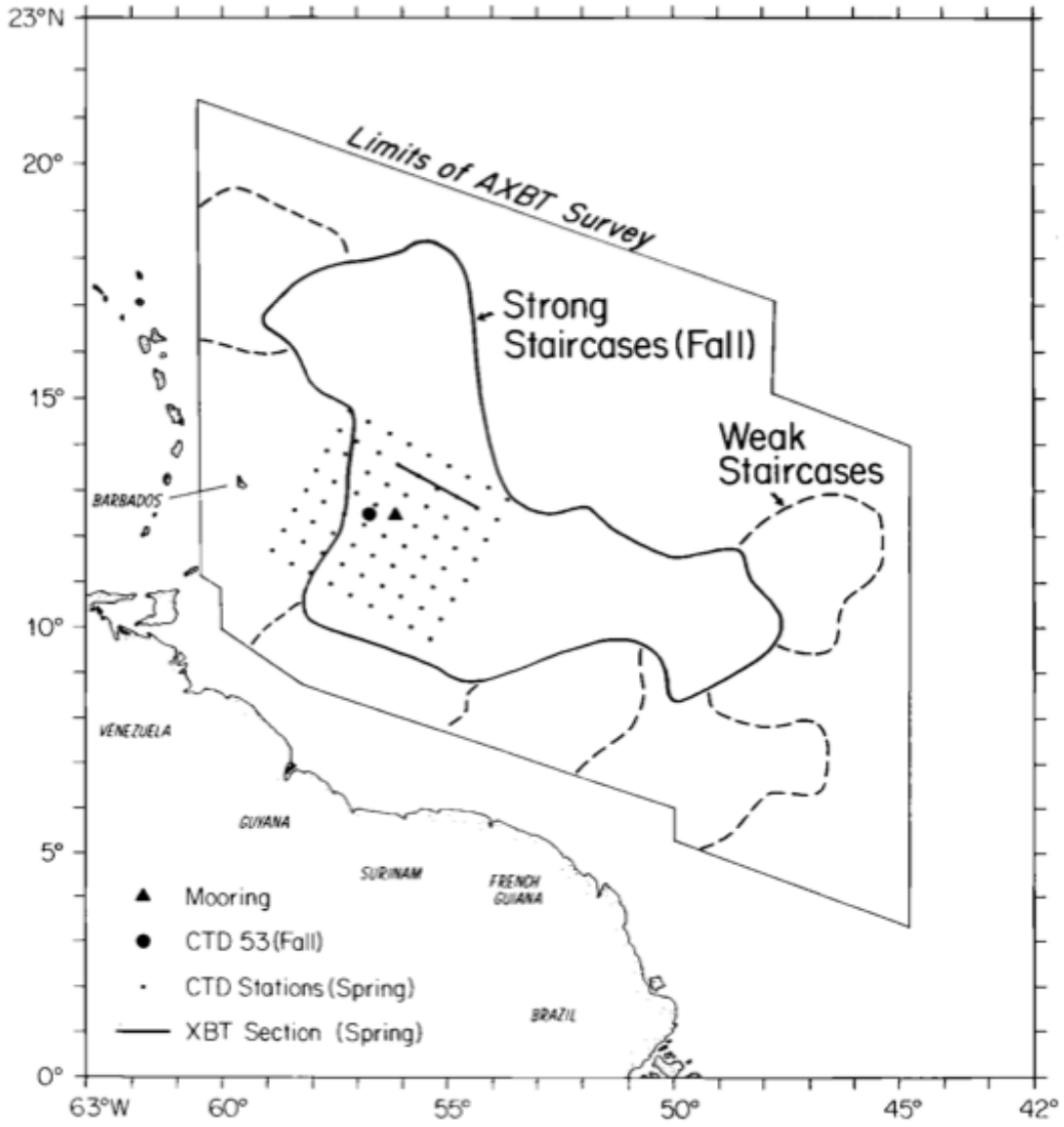

Figure 2. Area of C-SALT survey (From Schmitt, 1987)

It is this area that becomes the focus herein as we attempt to analyze, simulate and theorize the processes that occur within this staircase region, and conduct acoustic modeling through the staircases.

II. LATERAL COHERENCE, MERGING, AND ALIGNMENT OF THERMOHALINE STAIRCASES

A. LATERAL COHERENCE

1. C-SALT Observations

An interesting feature of the C-Salt observations was lateral coherence of the staircase layers over many kilometers by examining profiles at a variety of separations. The shortest separation between consecutive profiles was 1.3 km using a CTD tow-yo, covering a total distance of 33 km. The results of this are shown in Figure 3, whereby individual layers can be traced over the entire hydrographic section.

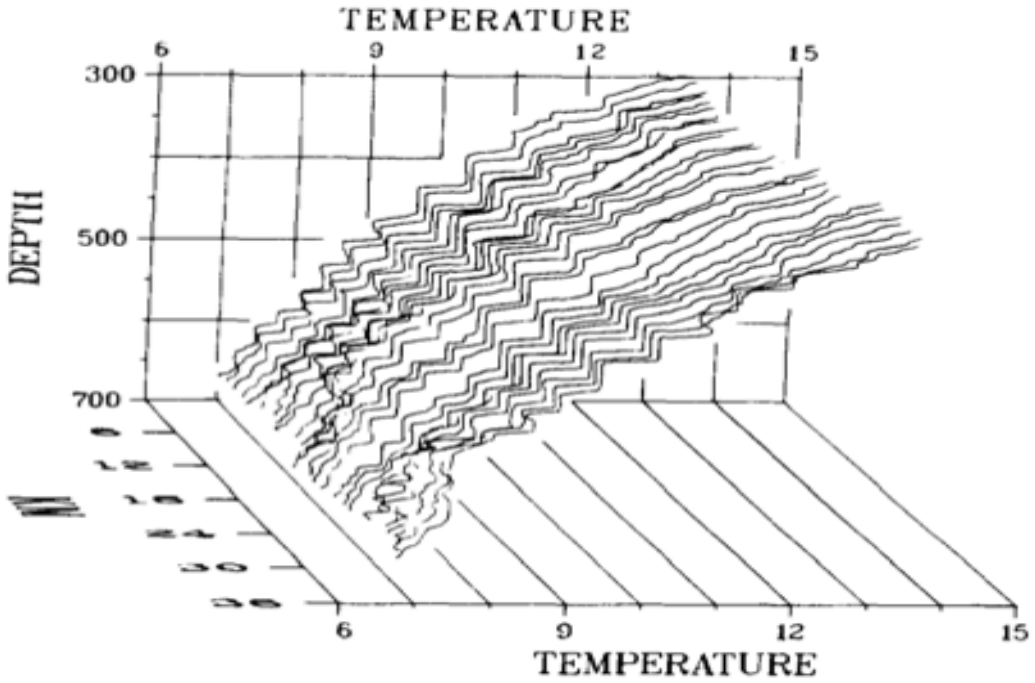

Figure 3. Three-dimensional view of CTD tow-yo (rear profile to the south) as the ship steamed to the north. 1.3 km separation between profiles, 33 km total distance covered (From Schmitt et al. 1987).

This lateral coherence was not limited to 33 km, as it was also measured in individual layers over a distance of more than 100 km using aerial dropped bathythermographs (XBT) spaced every 5.5 km in an east to west pattern (Figure 4).

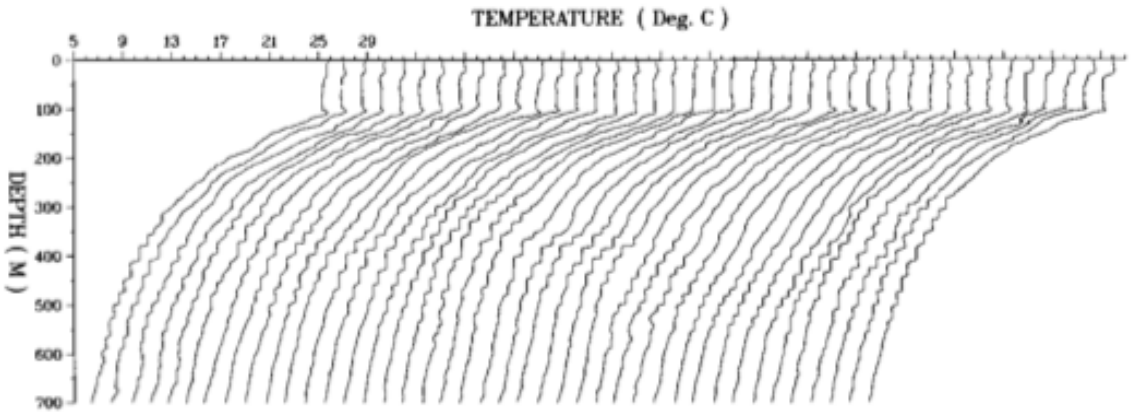

Figure 4. XBT temperature profiles from east to west, with 5.5 km separation between drops and total distance of 220 km. The profile at far left is correct, each subsequent profile is offset by 1.6 °c (From Schmitt 1987).

Over longer distances there were significant temperature and salinity changes within the layers, however an examination of the temperature and salinity characteristics of these layers produced a surprising pattern where temperature and salinity values are grouped in distinct lines, suggesting layers get warmer, saltier and denser to the north and west (Schmitt 1988). Figure 5 displays this unique grouping, which demonstrates that the well-defined slope of the layers crosses isopycnals. The horizontal density ratio, when averaged over the ten principle layers, was 0.85 (±0.02) in the spring, and 0.84 (±0.03) in the fall. Among other things, this value aided

in the realization that salt fingers were the dominant process in maintaining C-SALT staircases, as the value of the lateral density ratio was distinctly different from vertical mixing by small-scale turbulence ($R_\rho \approx 1.6$), and isopycnal eddy-stirring (1.0) (Schmitt 1988).

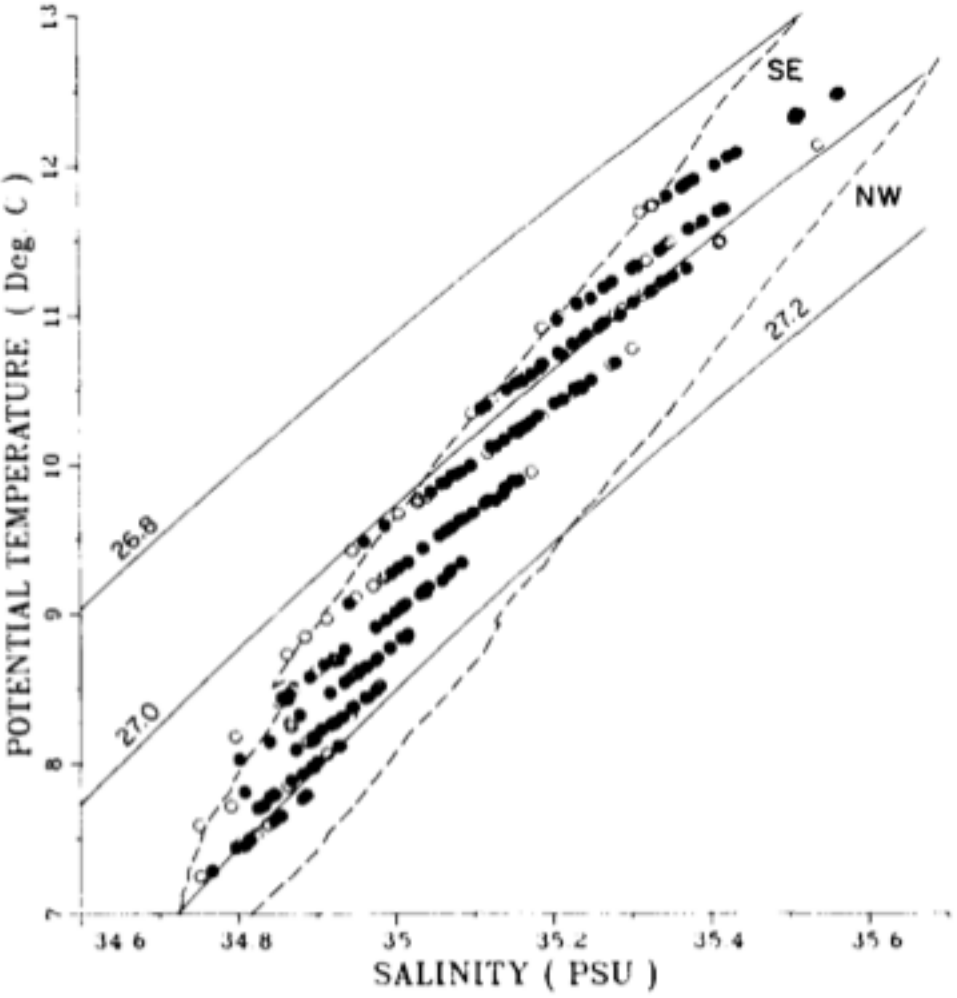

Figure 5. Potential temperature—salinity values of layers from CTD stations during C-SALT. Solid circles are from layers greater than 10 m thick, open circles are from layers 5–10 m thick. Hashed lines are temperature-salinity relationship obtained from stations at northwest and southeast corners of the survey. Solid lines represent isopycnal surfaces (From Schmitt 1987).

B. MERGING

1. Theory

It is difficult to gauge the evolution of layers in the C-SALT observations, short of saying that some staircases have persisted over 15 years, having again been observed in 2001 (Schmitt 2005). The evolution and long term persistence of these staircases can only be speculated, and the question remains as to whether they form over decades or centuries, and what, if anything, causes a collapse in the staircase. The theory behind staircase layer merging is explored here, and validated using a numerical model discussed later.

It has been proposed, and confirmed by direct numerical simulation (DNS), that layer formation occurs as a result of the instability of the heat/salt flux ratio, γ, that occurs when the flux ratio is a decreasing function of density ratio (Radko 2003). Further to this proposal is the theory that relatively thin layers within the staircase merge until the thickness of the layers exceeds a critical value, H_0, with equilibrium occurring as a result of inhomogeneity of the convecting layers stabilizing the staircase (Radko 2005).

In Radko (2007), a merging theorem was developed which states:

If the buoyancy flux decreases with the buoyancy variation across the step, then the staircase is affected by the B-instability, and the spontaneous merger of layers occurs through gradual erosion of weak interfaces. If, however, fluxes increase with step height, then coarsening

of a staircase may result from drift and collision of the adjacent interfaces. [Radko, 2007].

In Chapter III, we analyze the merging events in the numerical model, using the initial temperature of a layer at commencement of a merging event and the temperature variation in the layer during the event. In all simulations analyzed in this study, mergers occur following the B-merger scenario.

C. ALIGNMENT WITH BACKGROUND FLOW

Another area of research extending from the C-SALT experiment that was explored further by Wall (2007) was the alignment of the slope of staircase interfaces with the background large scale isotherms within the staircase region. Wall first began by considering a mixed layer sandwiched between two interfaces as shown in Figure 6, and starting with the conservation law for temperature and salinity in a mixed layer (F_{T2} and F_{T1} are the temperature flux at the top and bottom of the layer, respectively).

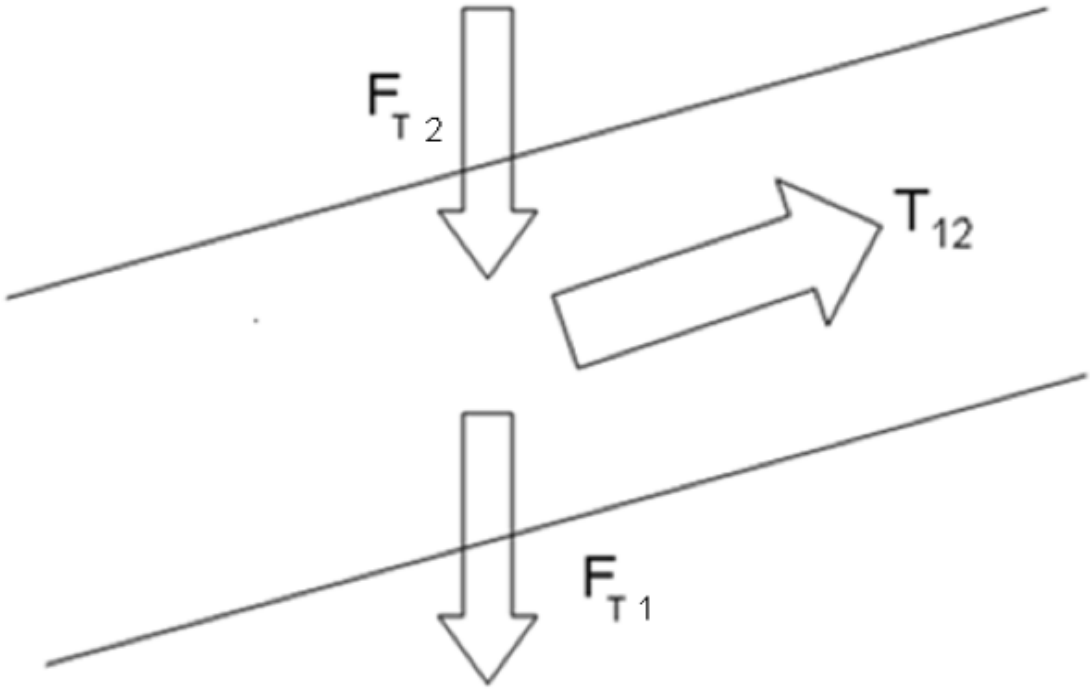

Figure 6. Basic two layer interface (from Wall 2007)

By adopting a co-ordinate system that is in the same direction as the flow, and using the Radko (2005) hypothesis that as a staircase evolves in time to a quasi-equilibrium state, the interfacial flux ratio approaches its minimum value, $\gamma_{\min}$, Wall arrived at the following:

$$\frac{(\partial T_{12} / \partial x)}{(\partial S_{12} / \partial x)} = \frac{(F_{T2} - F_{T1})}{(F_{S2} - F_{S1})} = \gamma_{\min} \qquad (3)$$

Wall rearranged the left hand side of this equation to be $(\frac{\partial T}{\partial S})_L$ and determined this value from the temperature-salinity plot similar to that shown in Figure 5 for stations in the C-SALT area exhibiting strong staircases. The temperature-salinity variation along the mixed layer was derived in terms of Cartesian derivatives and after a series of derivations Wall produced:

$$tg\alpha = (-tg\alpha_T \frac{\partial T}{\partial z} + \gamma_{\min} * tg\alpha_S \frac{\partial S}{\partial z}) / (\gamma_{\min} \frac{\partial S}{\partial z} - \frac{\partial T}{\partial z}) \quad (4)$$

$$tg\alpha = (-tg\alpha_T * R_\rho + \gamma_{\min} * tg\alpha_S) / (\gamma_{\min} - R_\rho) \quad (5)$$

where α_T and α_S are the slope of the background temperature and salinity, respectively, α is the slope of the layer interface, and assuming $R_\rho > \gamma_{\min}$ yields:

$$tg\alpha \approx tg\alpha_T \quad (6)$$

Wall thus hypothesized that the interface should align with isotherms but not necessarily isohalines. An observational test was carried out on the C-SALT staircases discussed above, using a numerical model based on the GFDL MOM3 code (Pacanowski and Griffies 1999) to determine the direction of the mean background flow. The results of this observational test showed a weak relationship in the direction of background flow between the isotherm and the slope of the layer (much less so in the case of isohalines). In the direction normal to background flow, the relationship between the isotherm and slope of the layer disappeared. This idea is further explored in the following chapter, in order to attain a stronger confirmation of this feature shown by Wall.

THIS PAGE INTENTIONALLY LEFT BLANK

III. SIMULATION OF STAIRCASES–EVOLUTION AND ALIGNMENT

A. MODEL SETUP

1. Massachusetts Institute of Technology General Circulation Model (MITgcm)

In order to simulate the staircases seen during the C-SALT field program, the MITgcm numerical model was chosen. The desirable features of this coupled model include, but are not limited to, the non-hydrostatic capability that allows the model to simulate fine, meso, and synoptic scale processes, and the ability to perform on a wide variety of computational platforms (Adcroft et al. 2012). The flexibility in building the model with varying parameters was ideal for the purpose of this investigation, where many parameters such as the horizontal and vertical diffusivity rates are not known, but can be slowly adjusted to produce simulations that reflect conditions in nature.

Model runs were performed on the Department of Defense High Performance Computing Modernization Program, Cray XE6 Open Research System (Chugach), located at ERDC, Vicksburg, Mississippi. 128 processors were used in coarse resolution grid simulations encompassing the entire ocean basin.

During early model initialization and simulation a coarse uniform 1 degree grid resolution was used over the entire ocean basin. Once this model had reached a period of perceived equilibrium at time = 18 yrs, a high resolution ($\Delta x = \Delta y = 10$ km) interpolation was carried out in the area of staircases, with the remainder of the ocean basin staying at coarse grid resolution. The simulation used $\Delta z = 1$

m and a Cartesian grid. Initial runs involved the use of the Gent McWilliams/Redi SGS eddy parameterization scheme (GMredi) which mixes tracer properties along isentropes (Redi 1982), and adiabatically rearranges tracers through an advective flux where the advecting flow is a function of the slope of the isentropic surface (Gent and McWilliams 1990). The GMRedi scheme was implemented using the tapering scheme of Large et al. (1997); however, it was found that over time the vertical temperature salinity profiles were smoothed to such an extent that the staircases were removed, an unexplained result in the simulation in direct opposition to what we know happens in the ocean. Thus the GMredi scheme was not used in most simulations.

Trial simulations were also carried out using various values of biharmonic diffusion coefficients, in order to accurately account for both mixing as a result of turbulence and double diffusion. The biharmonic diffusion coefficient was ultimately parameterized at $1*10^{-6}\ \ m^4/s$ over all 1000 vertical layers.

Various parameter adjustments were made throughout the course of model experimentation, and these are discussed later in the chapter.

2. Initial Datasets

At model initialization, temperature and salinity datasets were generated to provide a density ratio pattern over the tropical north Atlantic qualitatively resembling observations during C-SALT. The initial modeling of

temperature and salinity used in this experimentation at the surface and 1000m is shown along with density ratio values in Figure 7.

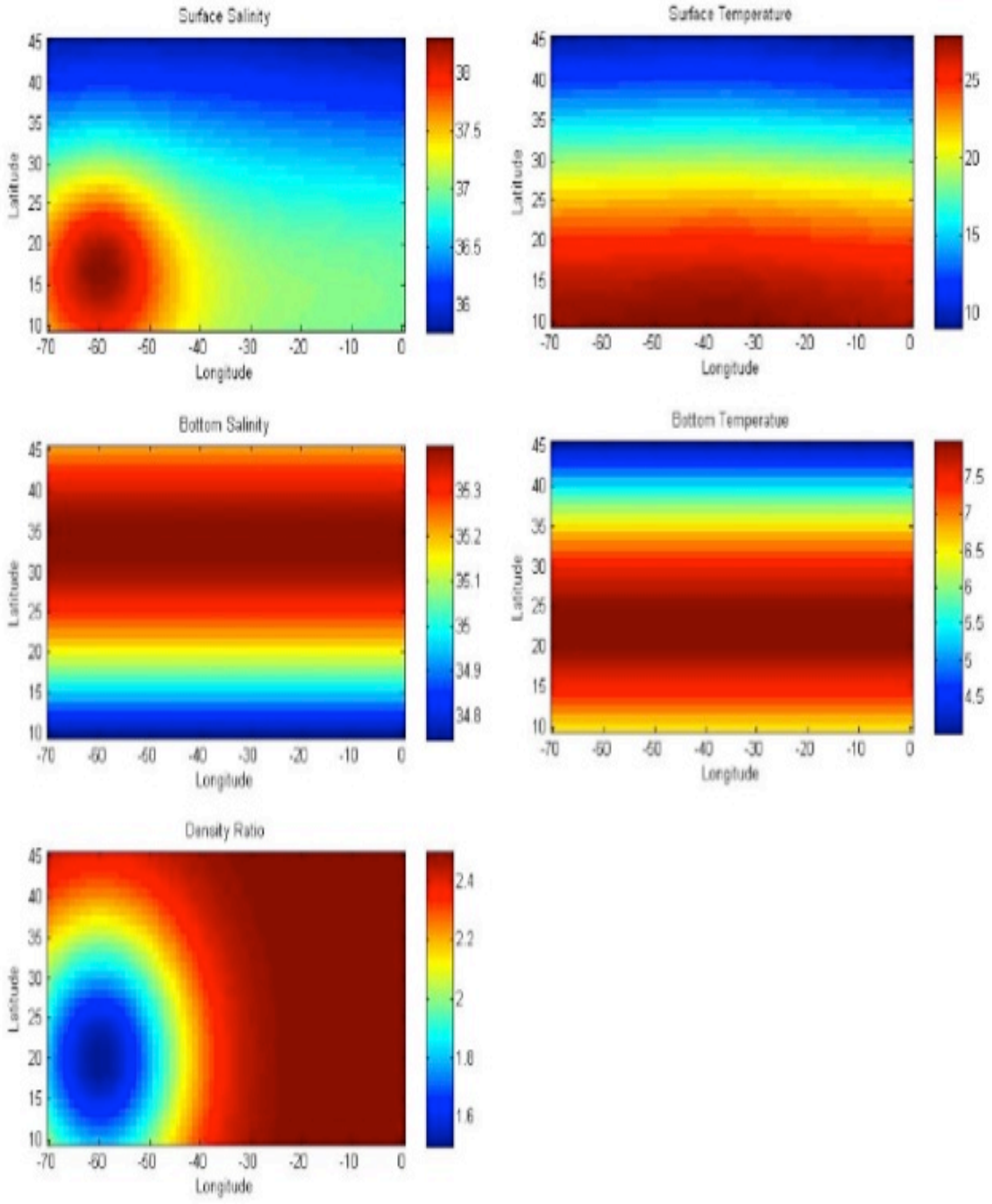

Figure 7. Temperature and Salinity at the surface and at 1000m depth, and Density Ratio, at initialization.

3. Model runs performed without Double Diffusion and with Constant Flux Ratio

In order to gauge the effect of double diffusion on the simulation, several model runs were conducted using different K profile parameterization (KPP) setups. The KPP scheme within MITgcm is a product of Large et al. (1994), and it unifies the treatment of a variety of unresolved processes in vertical mixing (Adcroft et al. 2012). The functionality to switch double diffusion on and off within the KPP scheme allows the ability to display a profile within the expected staircase region with and without double diffusive mixing, so as to see the effect double diffusion (and in this case, salt fingers) has on the development of staircases. Another useful feature of the KPP scheme in MITgcm is the ability to adjust the flux ratio. The flux ratio model used for all modeling is suggested by Radko and Smith (2012), who used high resolution DNS data to obtain the following algebraic expression:

$$\gamma = a_\gamma \exp(-b_\gamma R_\rho) + c_\gamma \tag{7}$$

where $(a_\gamma, b_\gamma, c_\gamma) = (2.709, 2.513, 0.5128)$. To illustrate the effects of using a variable flux ratio, another simulation was also conducted with a constant flux ratio of 0.5128. It is suggested in Radko and Smith that for the step-like patterns of thermohaline staircases to occur, the flux ratio must decrease with an increasing density ratio, in the oceanographically relevant range ($1 < R_\rho < 3$). We put this theory to the test by comparing these two simulations with

the expectation that with a constant flux profile a smoothed vertical temperature profile would be evident, as opposed to a flux ratio utilizing Equation 10, where a stepped vertical temperature profile would be expected. Figures 8 through 10 show a comparison of the varying KPP examples discussed here at time, t≈18 years, and it can be seen that the ideal KPP set up for growth and evolution of staircases similar to those observed in C-SALT is using the flux ratio at Equation 7 with double diffusion as a dominant vertical mixing process. Profiles are taken at the location $x = \frac{1}{3}L_x$ and $y = \frac{1}{4}L_y$, but the patterns are representative of the stratification in the entire domain.

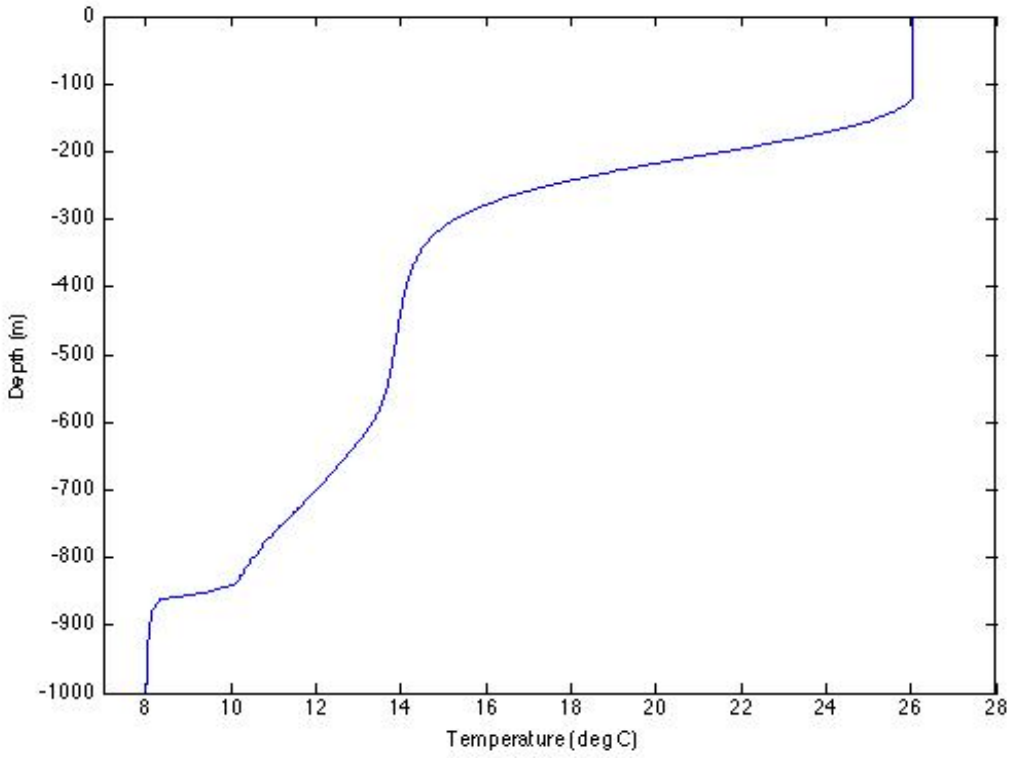

Figure 8. Vertical Temperature profile with constant flux ratio, $\gamma = 0.5128$.

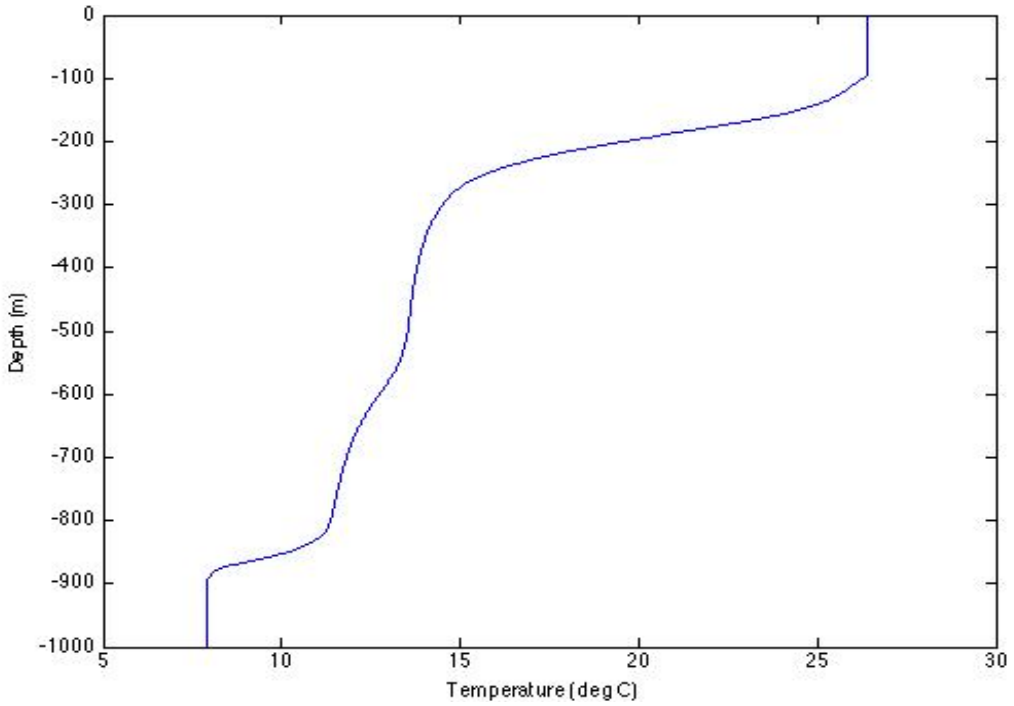

Figure 9. Vertical Temperature profile with the effects of double diffusion removed from the model.

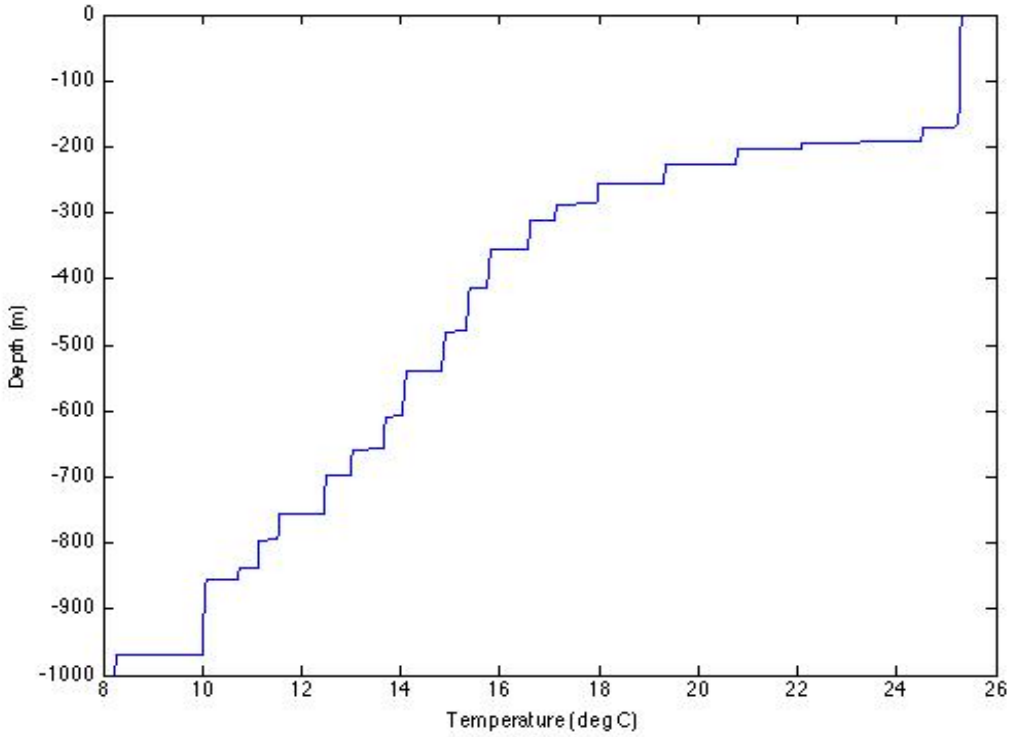

Figure 10. Vertical Temperature profile with flux ratio from Equation 10 and active double diffusion.

B. MODEL RESULTS

1. Effects of Vertical Eddy Diffusivities

Vertical eddy diffusivities due to small-scale turbulence, K_T and K_S, could be specified within MITgcm and typical oceanic values are of the order $10^{-5}\,m^2/s$. In order to examine the impact of turbulent diffusivities on thermohaline layering, the model was assigned a series of K_T and K_S values ranging from 0 to $10^{-4}\ m^2/s$, and then run to t≈18 years on each simulation. A Matlab code was developed to compare the staircase distributions with a two dimensional map of the density ratio, R_ρ, between 750 and 850 m. To identify staircase distributions, the average density ratio over the 100 m vertical section was calculated, and areas where density ratio changes within this area were greater than 10% of the average were identified:

$$\bar{R}_\rho = \frac{\max R_\rho - \min R_\rho}{1000} > \Delta R_\rho \qquad (8)$$

where $\bar{R}_\rho$ is 10% of the average density ratio and ΔR_ρ is the change in density ratio. If the individual density ratio change between 750 and 850 m was greater than 10% of the average density ratio change, and more than a third of the vertical profile (between 750 and 850 m) at individual points exhibited this characteristic, than staircases were deemed to exist at this location.

The results are displayed in Figures 11 through 14, where the white contours indicate the presence of thermohaline staircases. Alongside the staircase area is a graphical representation of the flux ratio dependence on

the density ratio at the specified eddy diffusivity. As per the suggestion by Radko and Smith (2012), thermohaline staircases are prevalent when the flux ratio decreases, but are almost non-existent when the flux ratio increases with increasing density ratio. It is evident that when K_T=2.5* 10^{-6} m^2/s and K_S=2.5*10^{-6} m^2/s, the numerical model closely replicates the observed density ratios and staircase formation areas of the C-SALT experiment, and at these regions the flux ratio is also decreasing. Other parameters that were adjusted to best replicate C-SALT observations are in Table 1.

Parameter	Value
Vertical Eddy Viscosity	$1*10^{-4}$ m^2/s
Lateral Eddy Viscosity	$2*10^{5}$ m^2/s
Lateral Eddy Diffusivity	$1*10^{2}$ m^2/s

Table 1. Parameter values in the numerical model.

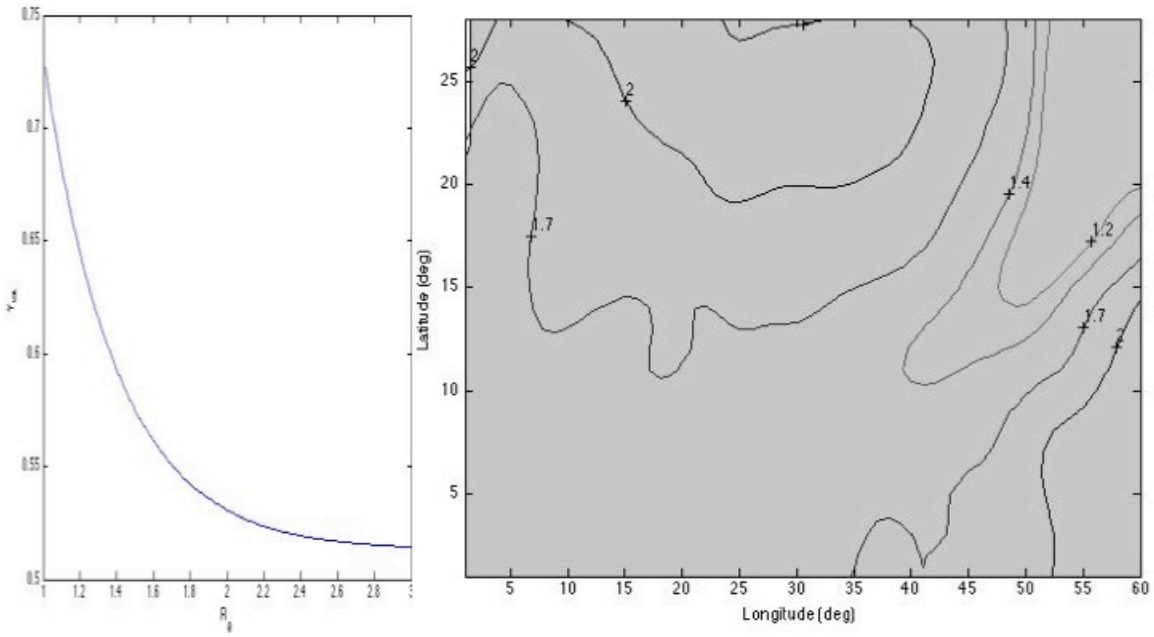

Figure 11. Total flux ratio versus density ratio (left) and density ratio (right) for $K_T = T_S = 0 \quad m^2/s$. Upon analysis staircases are evident throughout the region.

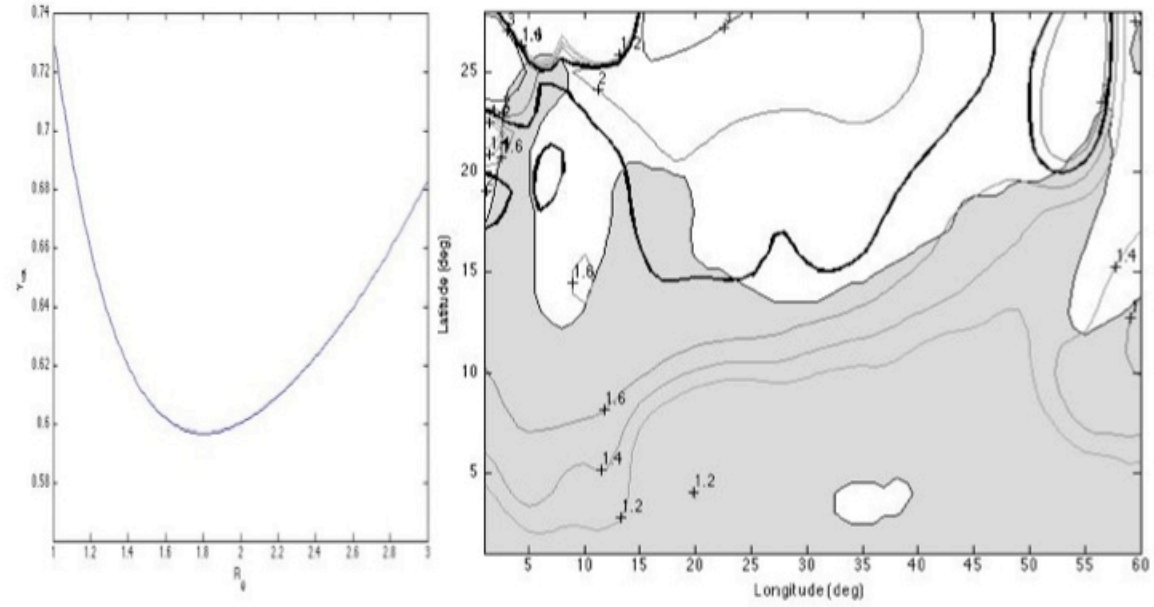

Figure 12. Total flux ratio versus density ratio (left) and density ratio (right) for $K_T = K_S = 10^{-6} \quad m^2/s$. Staircases are largely prevalent throughout the region as indicated by contours.

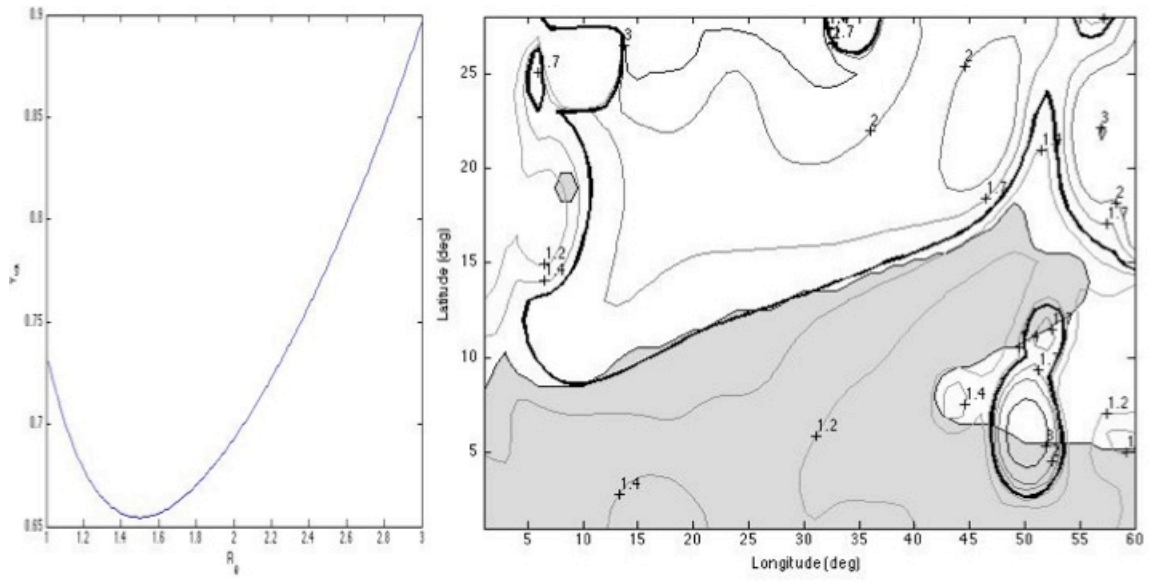

Figure 13. Total flux ratio versus density ratio (left) and density ratio (right) for $K_T = K_S = 2.5*10^{-6} \quad m^2/s$. Staircases are evident a region similar to that observed in the C-SALT experiment.

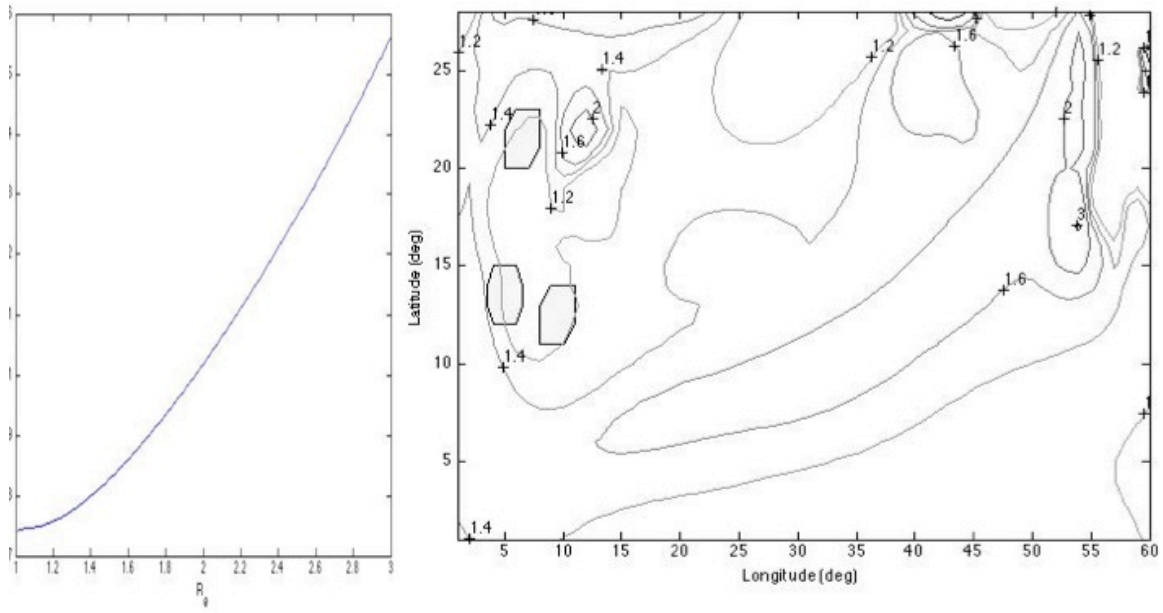

Figure 14. Total flux ratio versus density ratio (left) and density ratio (right) for $K_T = K_S = 10^{-5} \quad m^2/s$. Staircases are almost completely absent at this vertical eddy diffusivity.

2. Mechanism of Merging and Growth Rates

The model output was examined from initiation to perceived equilibrium. The images in Figure 15 through 17 represent a three dimensional visualization of the staircase looking north east from 50° West and 8° North between depths of 500 to 800 m shown at initialization of the model, an early point in the merging stage of the staircase, and fully matured merged layers. This three dimensional rendering is produced by VAPOR (www.vapor.ucar.edu), a product of the Computational Information Systems Laboratory at the National Center for Atmospheric Research.

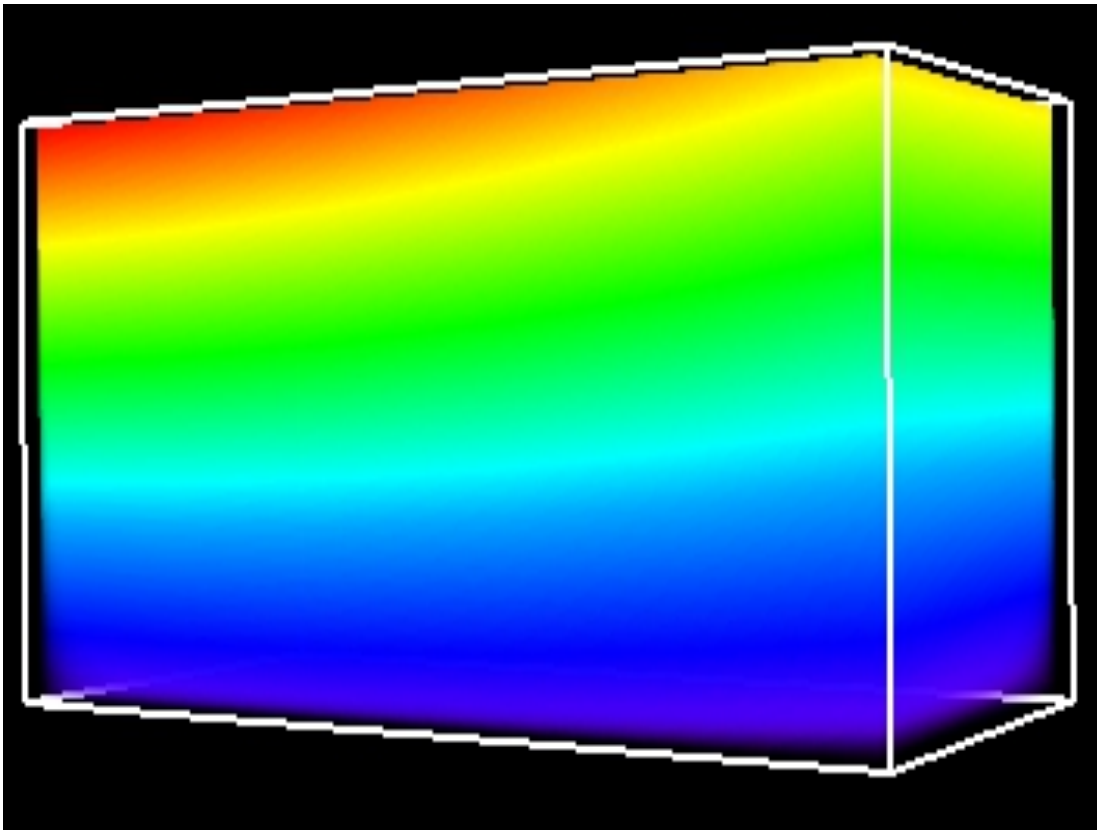

Figure 15. Three-dimensional visualization at t=0 secs.

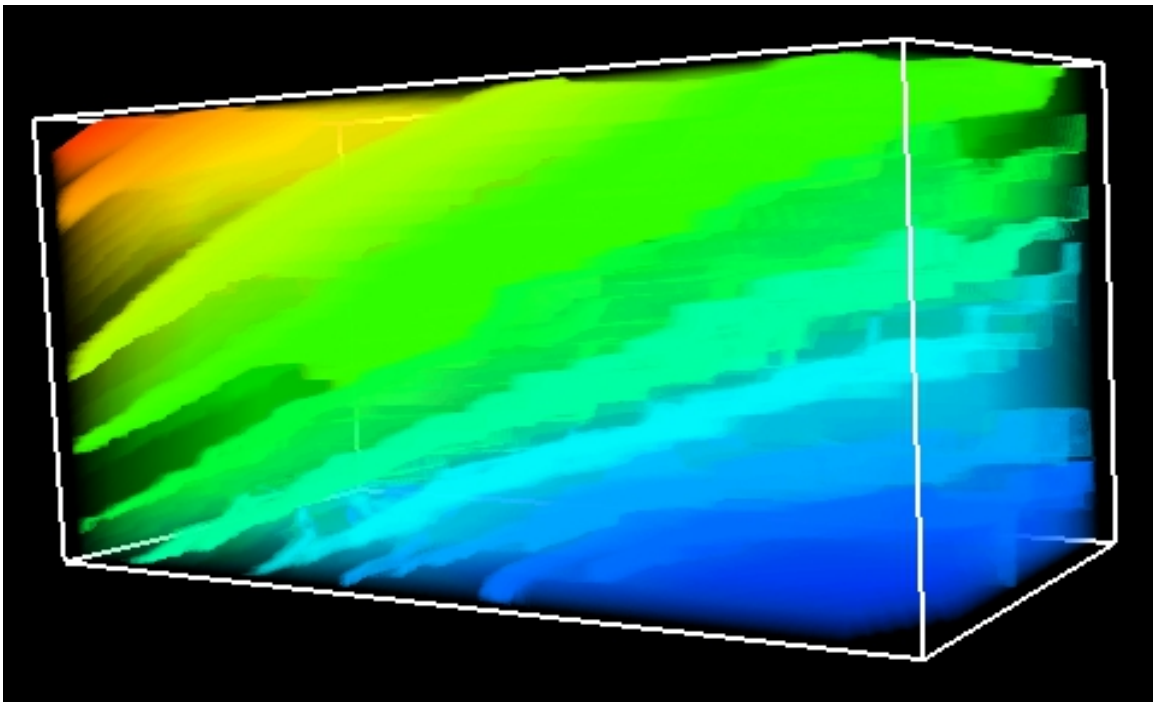

Figure 16. Three-dimensional visualization at t=10 years. Staircases are evident at this time and layers have commenced growth through merging.

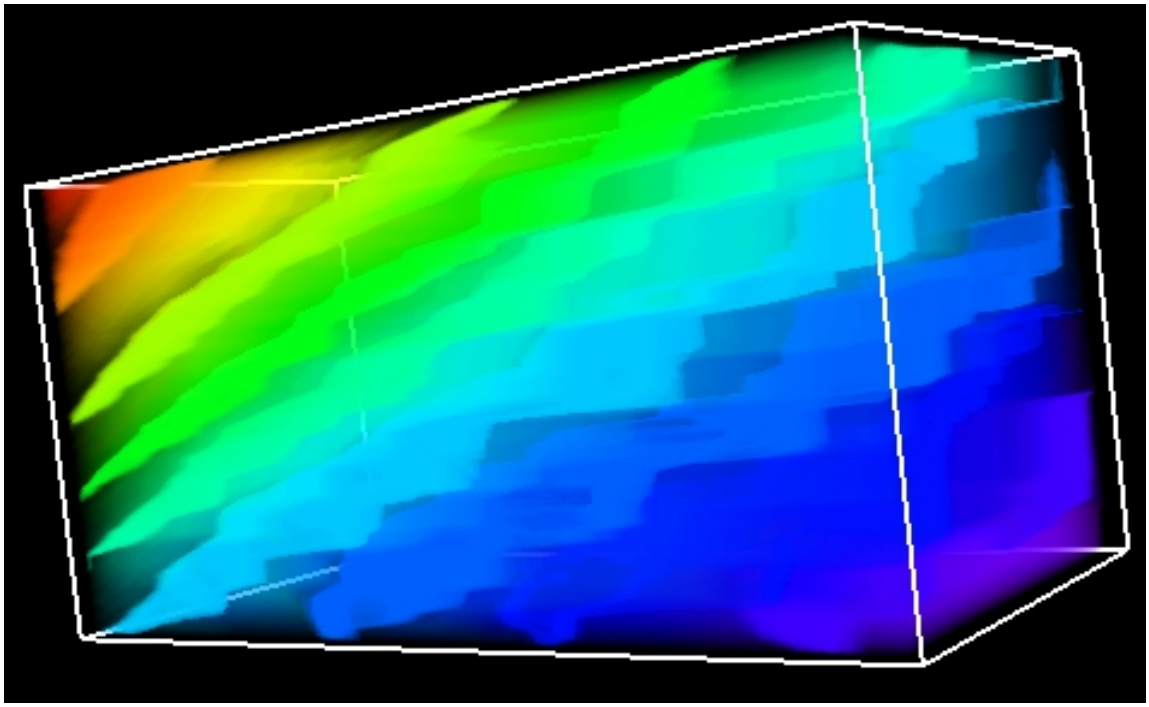

Figure 17. Three-dimensional visualization at t=18.6 years with evident staircases merged to equilibrium.

The evolution of the temperature profile in time is shown in Figures 18 and 19, from the initialization (t=0), the time t=5.4 years at which flux ratio instability modifies the initial profile, the time t=9.2 years where numerous density inversions are evidenced within the profile, to the point where a well-defined staircase is evident at t=10.4 years, and then several time steps illustrating the merging of the steps through to perceived equilibrium at t=18.6 years. Profiles are taken at the location $x = \frac{1}{3}L_x$ and $y = \frac{1}{4}L_y$, or 50° W, 8° N on a global grid.

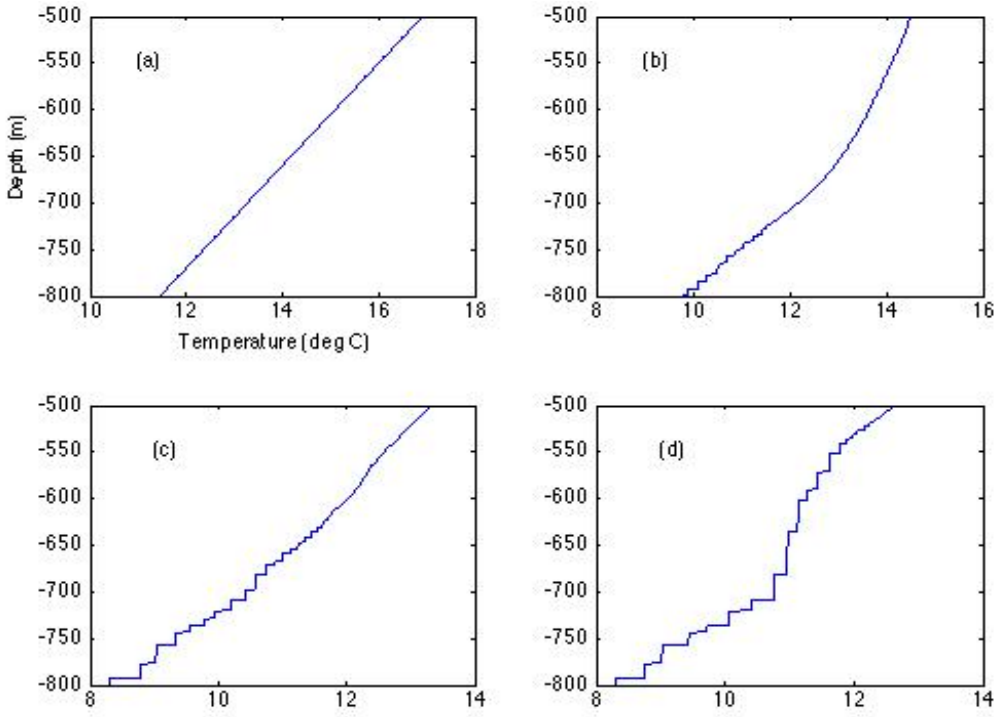

Figure 18. Formation and evolution of layers in the numerical model shown at (a-d) t=0, 5.4 , 9.2, 10.4 years.

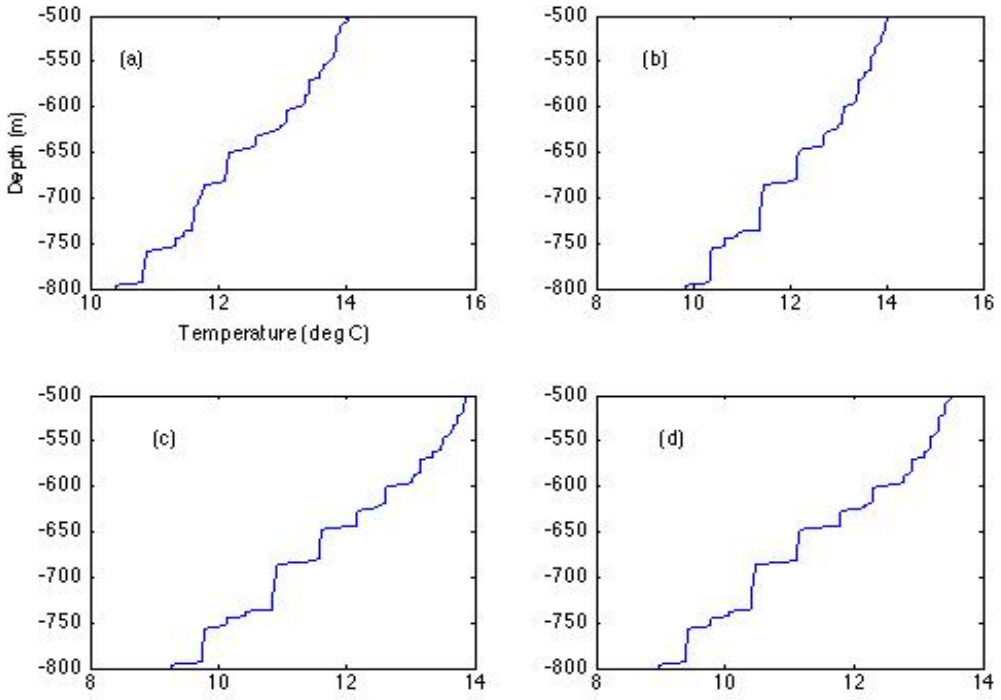

Figure 19. Evolution of layers in the numerical model shown at (a-d) t=14.7, 15.9, 17.7, 18.6 years.

The temperature gradient as a function of time is displayed in Figure 20, revealing the merging events over time. From this image it is evident that as the strong interfaces grow the weaker interfaces gradually decay and disappear (strong interface growth at the expense of the weaker interface, the B-merger as discussed in Chapter II).

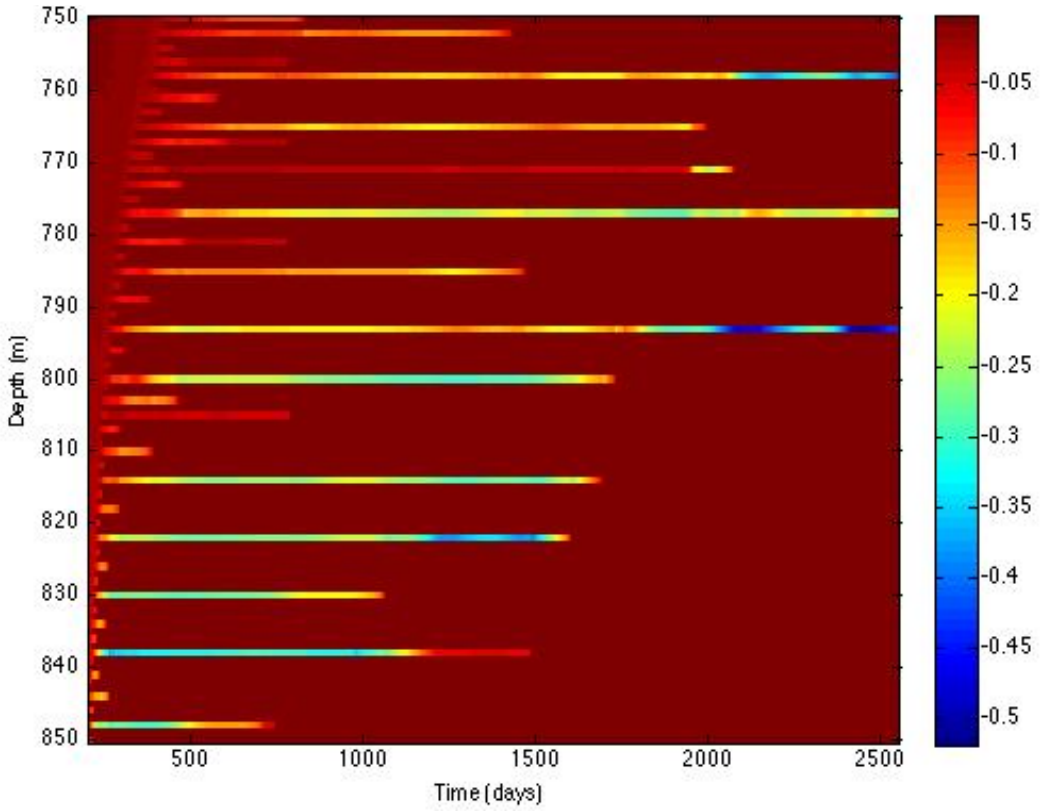

Figure 20. Space-time diagram of the numerically modeled temperature gradient ($^{\circ}c/m$). Layers merge when the relatively strong interfaces grow further at the expense of weaker interfaces, which decay and eventually disappear (B-merger scenario).

Essential insights into the layer-merging process brought by theoretical studies (Huppert 1971 and Radko 2005), is that the merging effect is a form of linear instability. Thus perturbations for a quasi-steady state are expected to grow exponentially. Our simulations offer a convenient opportunity to test these theories. Figures 21 and 22 show two separate merging events selected from the DNS over the time frame of the merge. The growth rate is exponential for both examples, which supports the theory merging as a result of linear instabilities.

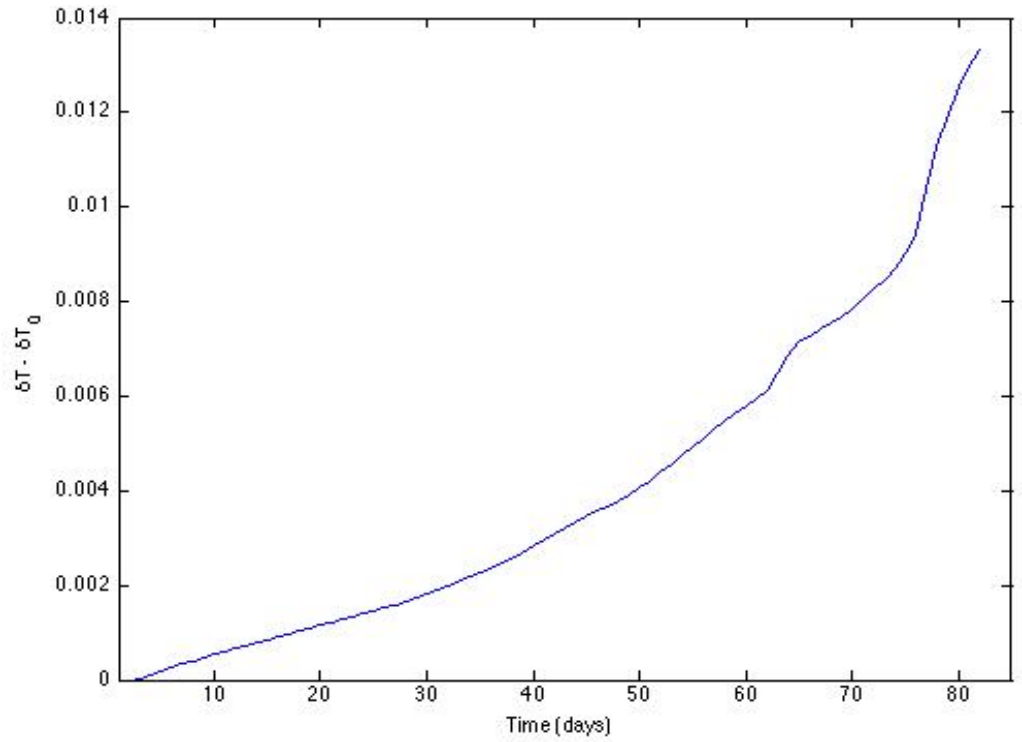

Figure 21. Change in temperature vs. time during merging event 1.

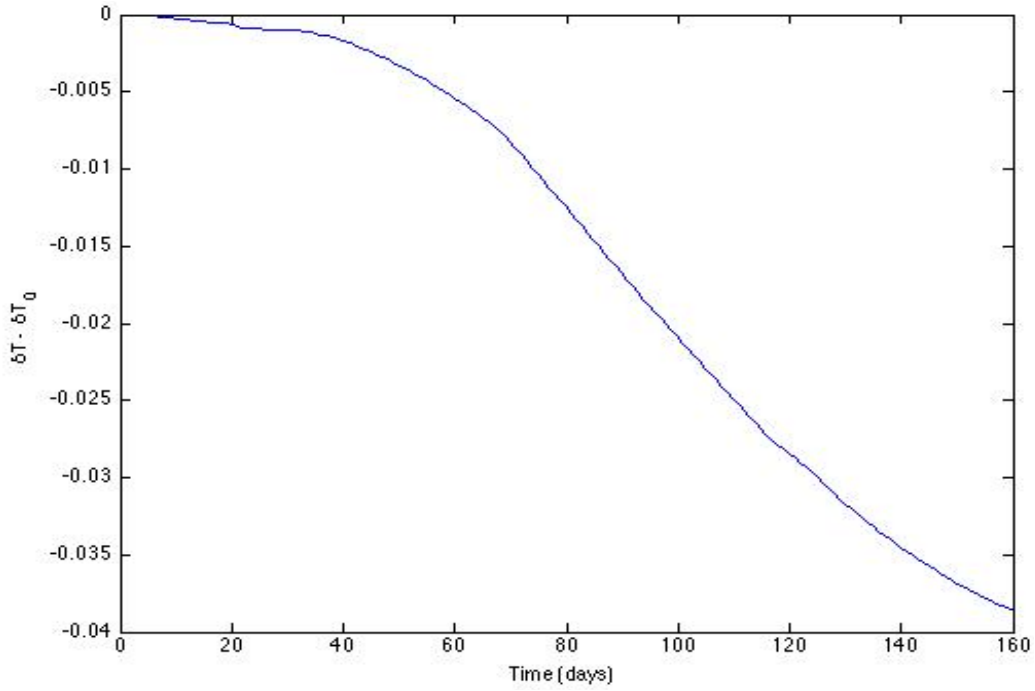

Figure 22. Change in temperature vs. time during merging event 2.

3. Lateral Coherence of Modeled Layers

Another feature of C-SALT that was also evidenced in the MITgcm simulation was lateral coherence of the layers over many hundreds of kilometers. The lateral extent of these layers within the simulation measured greater than 300 km with minor spatial changes in temperature and salinity within the layers as was also evidenced in C-SALT. Temperature and salinity data from three individual layers is plotted in Figure 23, and the result clearly portrays the layer temperature and salinity grouping aligned in a straight line with the layer slope crossing isopycnals, as it did during C-SALT (Figure 5). It is noted that this pattern became more pronounced as horizontal eddy diffusivities, $K_h T$ and $K_h S$ decreased by O(10), from 1000 to 100 m^2/s. The average density ratio was defined by the temperature and salinity changes and was calculated to be 2.01, and the resultant theoretical flux ratio using the equation of Radko and Smith is 0.53. The line of this slope is shown in Figure 23 below each set of layer points to show the correlation between the flux ratio and lateral density ratio.

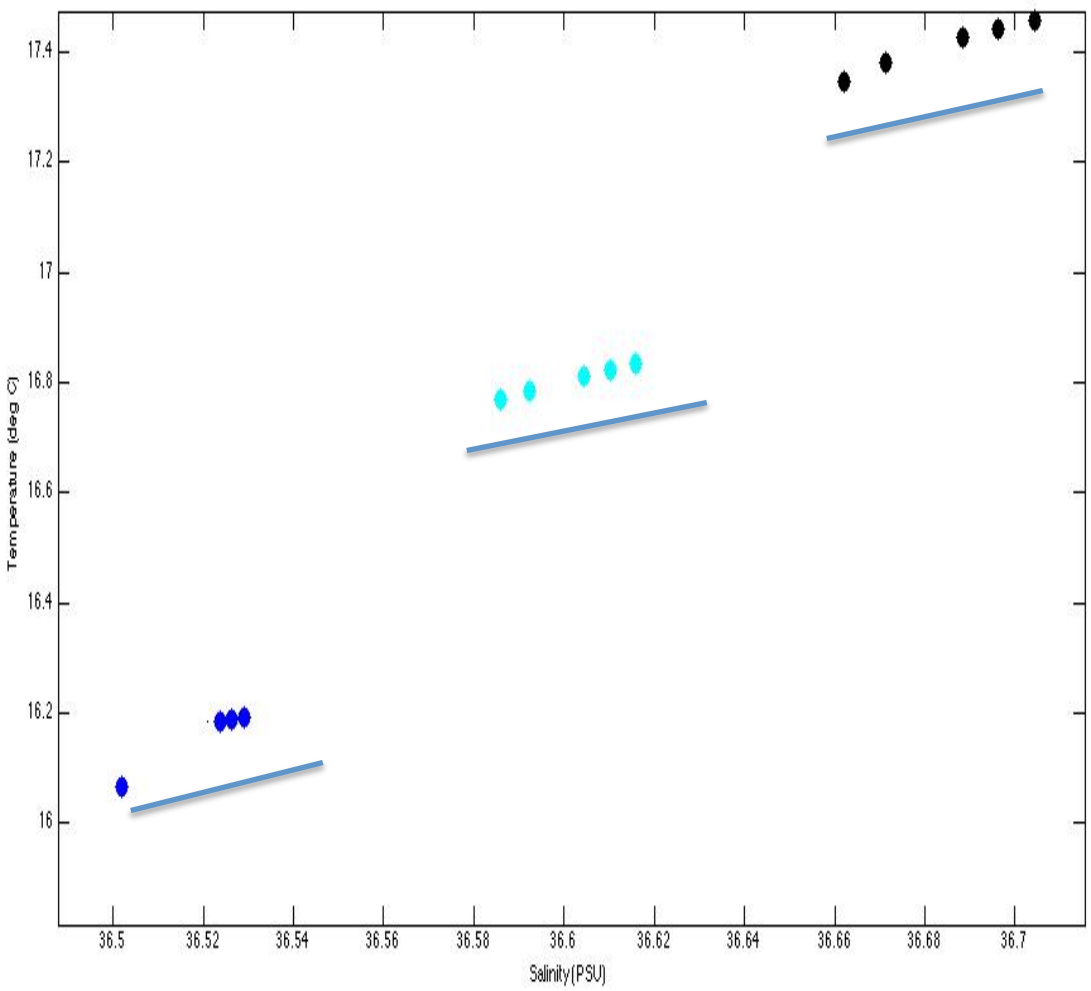

Figure 23. Temperature-salinity values taken from three individual layers in the model. Each color represents a separate layer.

The lateral coherence is clearly displayed in Figures 24 and 25, which show a series of vertical temperature profiles from the numerical model taken in the C-SALT area at horizontal separation of 10 km in the east-west direction, covering a total distance of 290 km. The temperature scale is correct for the far left profile, with each consecutive profile offset by 1.6 $^{\circ}C$. Individual layers can be traced along the entire distance, displaying a very clear lateral coherence, which extends over 300 km.

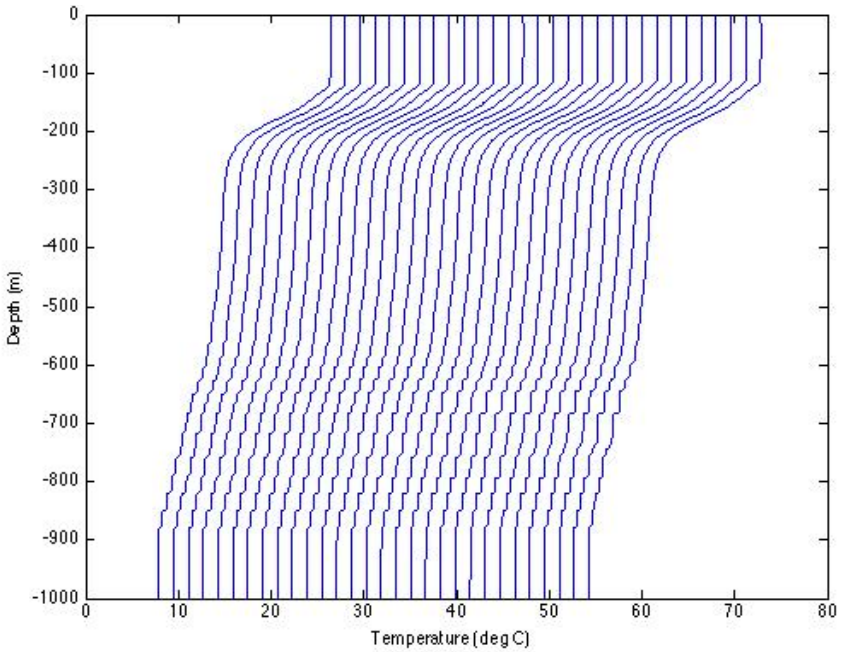

Figure 24. Series of offset temperature profiles from the DNS in an east to west section with 10 km separation. The right-most profile lies to the east of the others; the total distance covered is 290km. The temperature scale is correct for the left-most profile and each subsequent profile is offset 1.6 $^{\circ}C$.

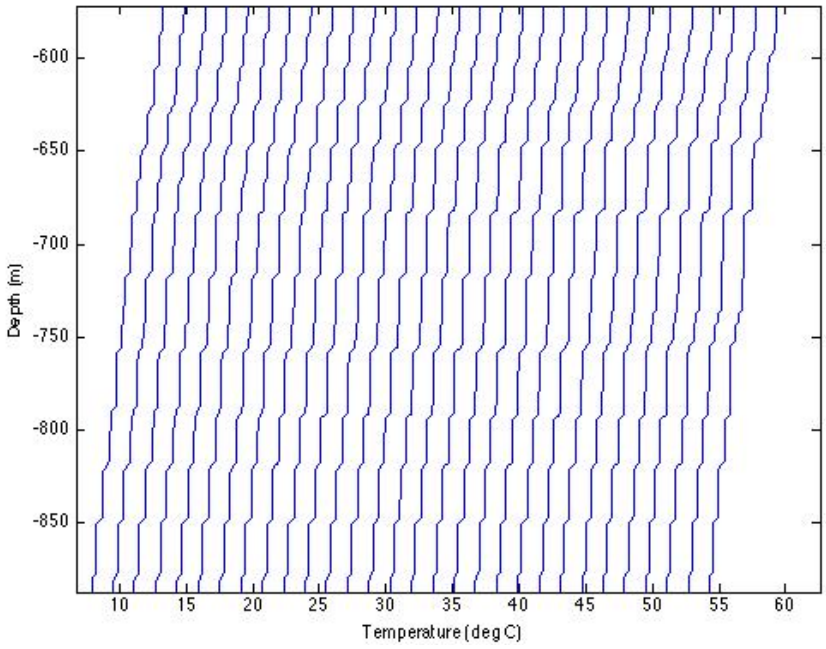

Figure 25. Temperature profiles from Figure 24, focused at the depth of staircase formation.

4. Alignment of Interface Slopes with Background Flow

To attempt to correlate the slope of the interface with the background flow as discussed in Chapter II, the background flow must first be found. A Matlab code was run to identify the lateral temperature and salinity, T_l and S_l, along the direction of the flow using the following formulation, where u and v are velocity in x and y, respectively, in a Cartesian grid:

$$T_l = T_x \frac{u}{|\vec{V}|} + T_y \frac{v}{|\vec{V}|} \tag{9}$$

$$S_l = S_x \frac{u}{|\vec{V}|} + S_y \frac{v}{|\vec{V}|} \tag{10}$$

The slope of the isotherm and isohalines can then be defined as:

$$tg(\alpha_T) = \frac{T_l}{T_z}$$
$$tg(\alpha_S) = \frac{S_l}{S_z} \tag{11}$$

The mean background flow was found to be predominantly West South West in the DNS throughout the C-SALT area of interest. The intent was to determine the slope of the interface by identifying the layer, and then determining the gradient change. Unfortunately, as can be viewed in the lateral coherence figures, the depth change of the layers was exceptionally small over several hundred kilometers (layers are almost completely horizontal). This results in a zero degree angle for the interface, therefore the following explanation of the continued analysis is provided for future research purposes.

Using Wall's formulation for the interface slope (Equation 7), the theoretical value can be compared with the numerical simulation. Taking Equations 9 and 10 and shifting 90 degrees to the right to evaluate normal flow gives:

$$T_n = T_x \frac{v}{|\vec{V}|} + T_y \frac{(-u)}{|\vec{V}|}$$
$$S_n = S_x \frac{v}{|\vec{V}|} + S_y \frac{(-u)}{|\vec{V}|} \qquad (12)$$

where the numerator in Equations 13 and 14 is now given to be T_n and S_n, respectively. It is proposed that this can also be compared with the interface angle to demonstrate a lack of correlation between interface slope and isotherms or isohalines normal to the direction of flow.

THIS PAGE INTENTIONALLY LEFT BLANK

IV. STAIRCASE EFFECTS ON ACOUSTIC PROPOGATION

A. BACKGROUND

The effect of thermohaline staircases has previously been studied, both within the C-SALT area and in other areas of the ocean. Chin-Bing et al. (1994) used data that was collected from the northeast coast of South America adjacent to the C-SALT area in 1985. These staircases were formed as a result of salt-fingering. The study focused on the effect of the sound velocity profile as a result of the staircases, and resultant acoustic propagation simulations. The study only investigated the effect at 50 Hz, which creates an acoustic wavelength of similar size to the step size. A conclusion from the study was that for significant differences in prediction to be observed both the source and receiver needs to be placed within the depth range of the staircases.

Wall (2007) built on this investigation of acoustic propagation using a parabolic equation (PE) model for a stepped profile taken from C-SALT. The PE model was run using two different source depths (one within and one below the staircase region), and three different source frequencies. Contrary to Chin-Bing's findings, Wall found that the source and receiver did not need to be at the same depth as the stepped layer for significant differences to be observed between a smooth and stepped profile acoustic prediction. This finding was similar to one found in the past by Wilson (2007), who studied propagation through a stepped structure resultant from diffusive convection. Wall also found that as the frequency of the source is increased

the effect of the staircase on the acoustic prediction is amplified. A limitation to these observations was frequency, where 1200Hz was the highest frequency studied.

This study continues to build on Wall's observation, using a different model (Bellhop) to compare past results, and increasing the frequency to determine if the decrease in wavelength continues to have an impact on difference in acoustic prediction between smooth and stepped profiles taken from C-SALT. The analysis of the source within the staircase is investigated further than the previously mentioned studies, such that the source is set at a depth corresponding to a prominent interface, and also at the center of a prominent mixed layer to determine whether the positioning of the source within the staircase region plays a pivotal role in the propagation. Based on the findings of lateral staircase alignment in earlier chapters, an acoustic prediction is carried out over a range dependent simulation to assess how laterally coherent staircases impact acoustic propagation.

B. PROCESS

The Bellhop model is a beam tracing model for ocean acoustic predictions. The theory behind the ray equation used in Bellhop can be expressed as:

$$\begin{aligned} \frac{dr}{ds} &= c\xi(s) \\ \frac{d\xi}{ds} &= -\frac{1}{c^2}\frac{\partial c}{\partial r} \\ \frac{dz}{ds} &= c\zeta(s) \\ \frac{d\zeta}{ds} &= -\frac{1}{c^2}\frac{\partial c}{\partial z} \end{aligned} \tag{13}$$

where r(s) and z(s) represent ray coordinates in cylindrical coordinates, s is the arc length along the ray, and c(s)[ξ(s),ζ(s)] represents the tangent versor along the ray. Initial conditions for r(s), z(s), ζ(s) and ξ(s) are

$$\begin{aligned} r(0) &= r_s \\ z(0) &= z_s \\ \xi(0) &= \frac{\cos\theta_s}{c_s} \\ \zeta(0) &= \frac{\sin\theta_s}{c_s} \end{aligned} \tag{14}$$

where θ_s represents launching angle, (r_s,z_s) is the source position, and c_s is sound speed at source position. The coordinates are sufficient to obtain the ray travel time:

$$\tau = \int_{\Gamma} \frac{ds}{c(s)} \tag{15}$$

calculated along the curve [r(s), z(s)] (Rodriguez, 2012).

To run the desired profiles through the Bellhop model an environmental file first needs to be created. Data from a C-SALT CTD (Conductivity Temperature Depth) probe from station 20 ($14°12.70$ N $56°17.60$ W) that displayed significant staircase development was used, as was the MITgcm modeled simulation of laterally coherent well-developed staircases, the temperature profile of these examples is in Figure 26. The sound speed profile (SSP) was calculated using MATLAB code from the seawater toolbox, and is displayed in Figure 27. The small increase in sound speed at the base of individual layers in the staircase region SSP is expected

due to the isothermal feature, and increasing depth (and hence pressure), of the layers within the staircase.

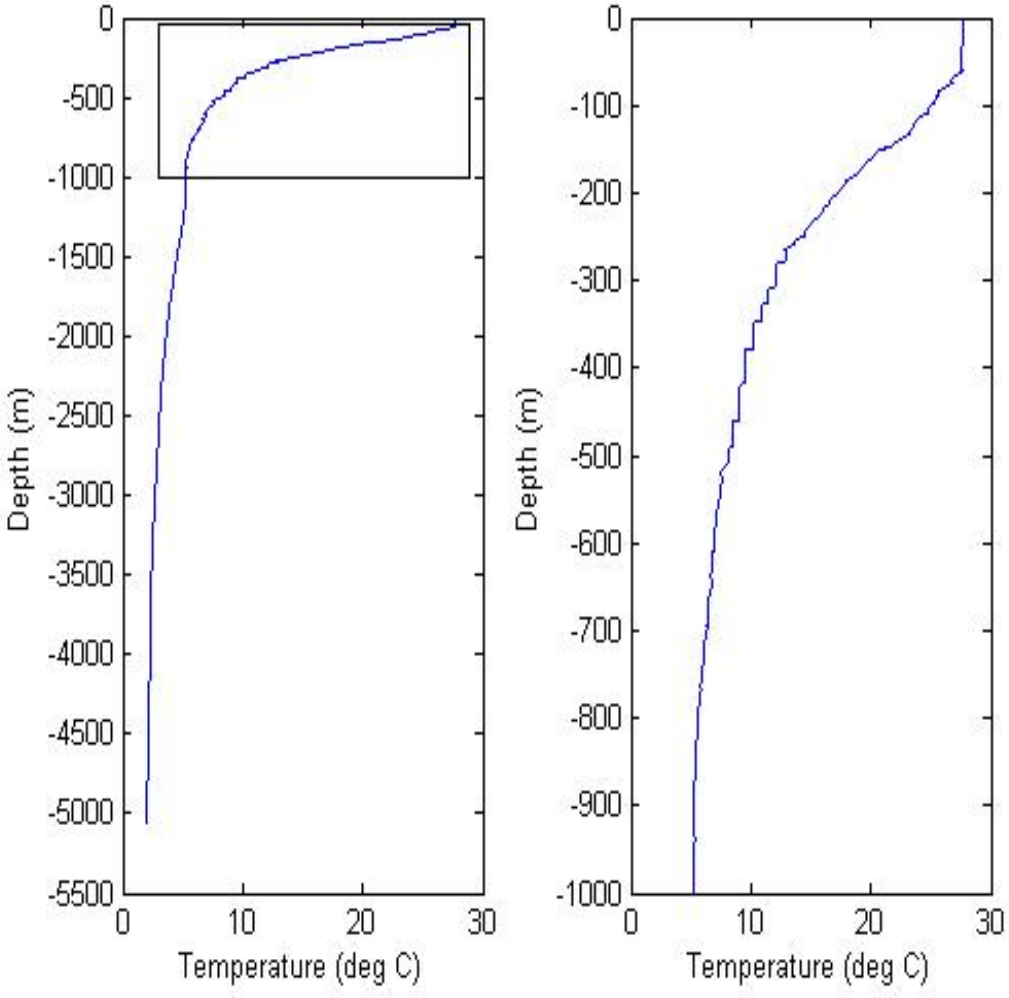

Figure 26. C-SALT Station 20 Temperature profile (left) with upper 1000m displayed (right).

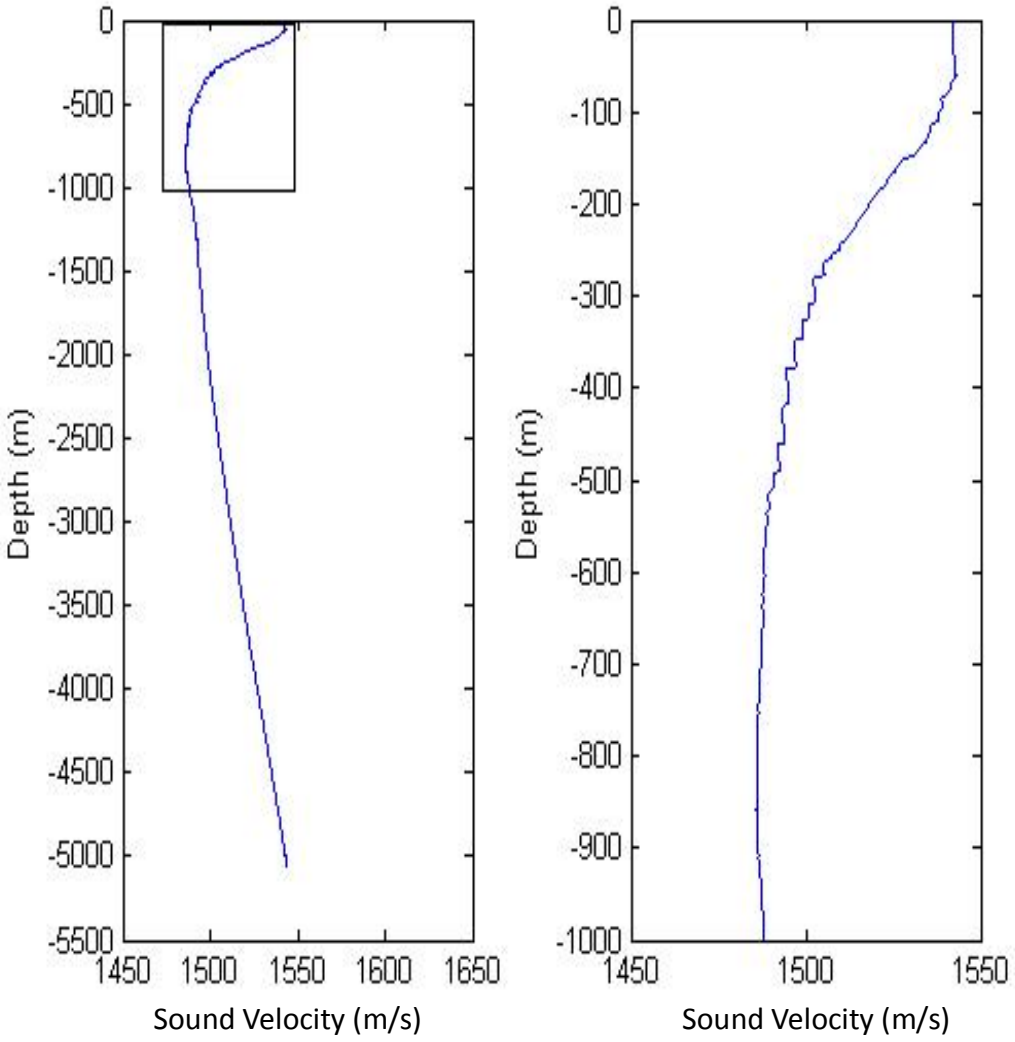

Figure 27. C-SALT Station 20 SSP (left) with upper 1000 m displayed (right).

The C-SALT SSP was also smoothed to remove the sharp changes in sound speed due to the staircase, using a low pass moving average filter with a span of 41 points, and this profile was used as the example of an ocean environment without staircases, and is in Figure 28 and 29.

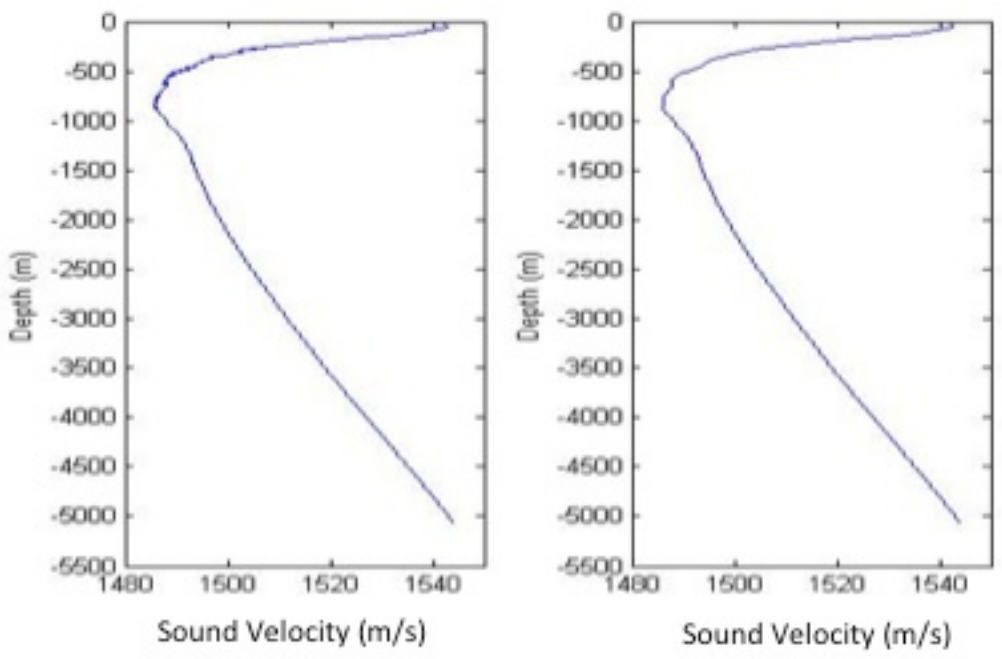

Figure 28. C-SALT Station 20 SSP (left) and smoothed profile (right).

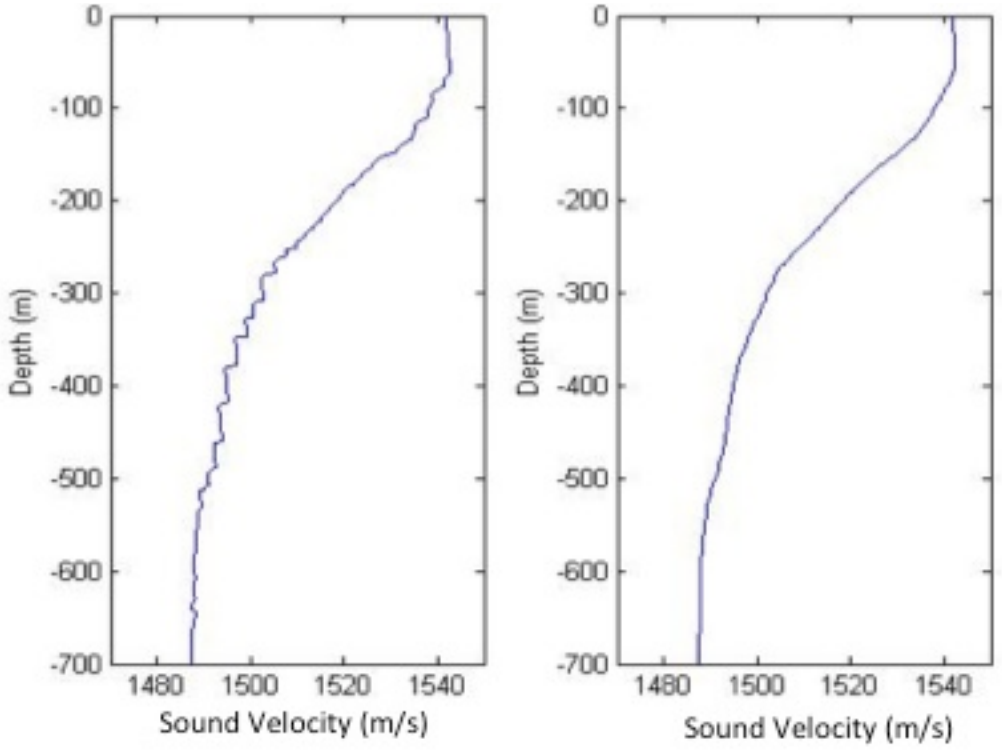

Figure 29. C-SALT Station 20 SSP to depth 700 m (left) and smoothed SSP to depth 700 m (right)

When building the environment file, only 1000 m of data was used, with the bottom type acting as an acoustic half-space, with a 1.8 g/cm^3 density and attenuation coefficient of 2 dB/m. The attenuation coefficient was chosen using Figure 17 of Hamilton (1980), to be just above the attenuation value expected for compressional waves versus frequency in natural, saturated sediments and sedimentary strata, for the frequency range which we are focused on (up to 5 kHz). The reasoning behind this was to absorb as much sound as possible into the "false" bottom, so as to reduce the impact reflected or refracted rays re-entering the staircase region from the bottom may have on the acoustic propagation.

The scenarios presented in part b are conducted over three source depths: 5 m, 387 m and 450 m. 5 m is a typical depth of a fixed hull mounted sonar, and thus provides a good representation of a source outside of staircase depths. 378 m is the depth at which a rather prominent layer interface occurs in the C-SALT profile, and 475 m is close to the vertical center of a layer within the staircase region. All source depth scenarios were evaluated at frequencies of 50 Hz, 2000 Hz, and 5000 Hz to evaluate the effect of the deep layers on smaller wavelengths.

C. RESULTS

1. Source Depth 5 m

a. Ray Trace

With both the smoothed and stepped profile the ray trace (Figure 30) appears the same, regardless of frequency. This is largely to be expected as both smoothed

and stepped scenarios display the same profile to a depth of 250 m, at which point the staircase is introduced. Thus a source near the surface experiences surface ducting due to the mixed layer, and then a downward refracting ray trace due to the decreasing sound speed profile, with a shadow zone between the duct and the downward refracted rays. The staircase has little impact on this ray trace, as the layer depth is not large enough to result in a significant refractive change in the overall downward ray trace pattern.

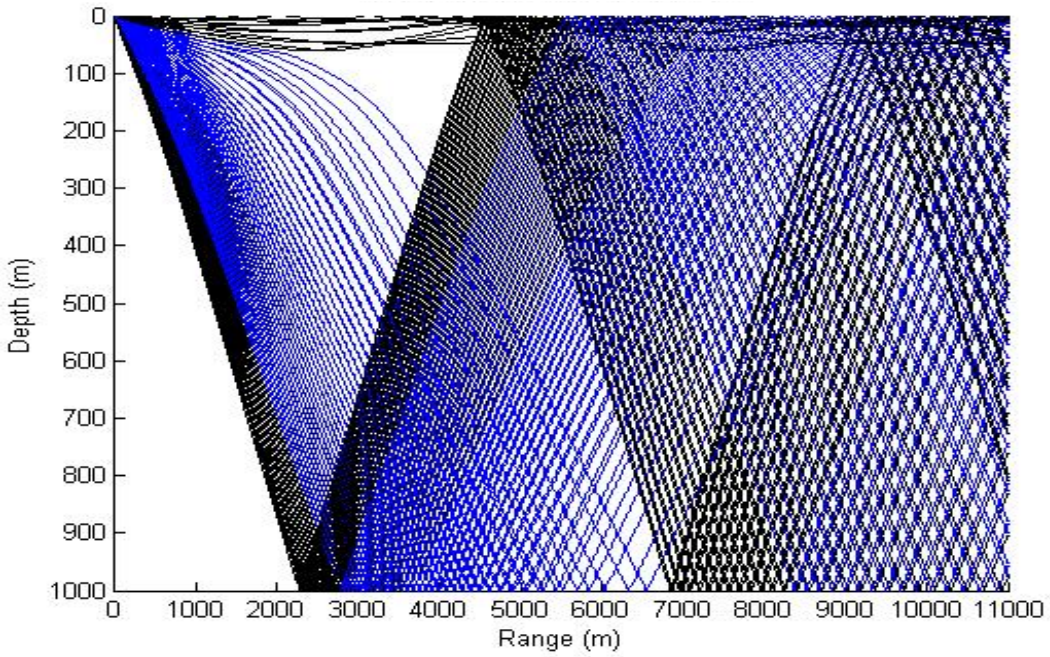

Figure 30. Ray Trace profile for a source at 5 m in a staircase environment. The ray trace is nearly identical to that which occurs for a smoothed profile.

b. Transmission Loss

At a source depth of 5 m, there was no difference in the transmission loss between a stepped and smoothed

profile. The results were the same as frequency increased. Figures 31 and 32 show the transmission loss experienced by both profiles at 2000 Hz. This result is contrary to the findings by both Wilson (2007) and Wall (2007), which stated the source could be outside of the staircase region and have a significant effect on propagation.

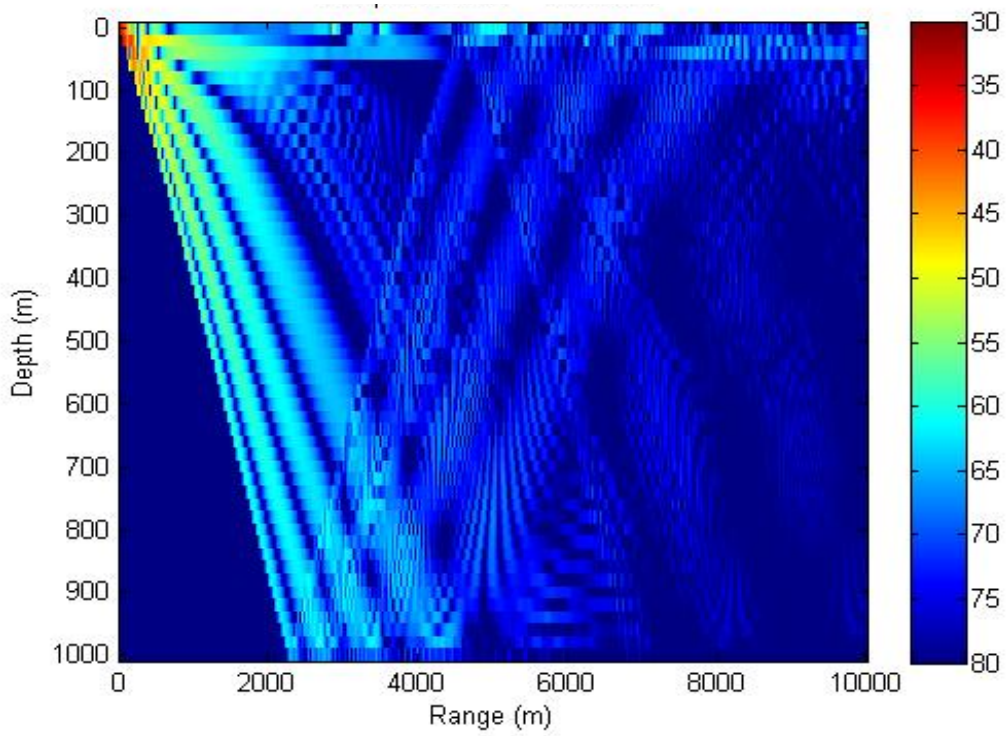

Figure 31. Coherent transmission loss (dB/m) for a source at 5 m depth and 2000 Hz frequency for a smoothed environment.

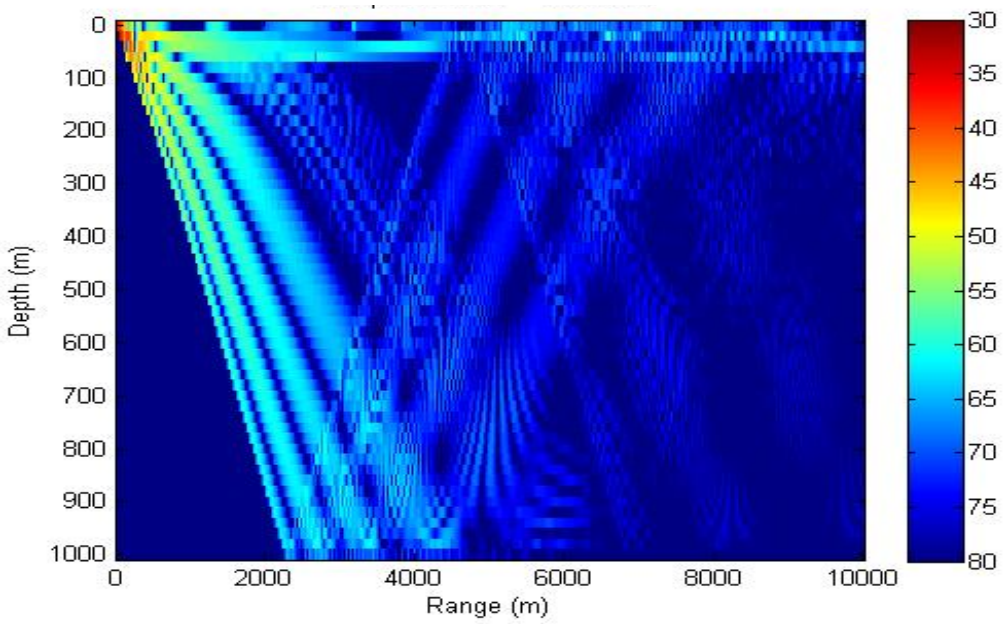

Figure 32. Coherent transmission loss (dB/m) for a source at 5 m depth and 2000 Hz frequency for a stepped environment.

2. Source Depth 387 m

a. Ray Trace

The ray trace for a source at 387 m is significantly different between the smooth and stepped profile as seen in Figures 33 and 34. At this depth, the source lies at an interface for the stepped profile, but in the smoothed profile at this depth the SSP continues to decrease. It is evident that when the source lies at the same depth as an interface in a region of staircases, there is a significant divergence of the rays at this point. For low launch angles the rays refract upward or downward, leaving a rather significant shadow zone horizontally in front of the source.

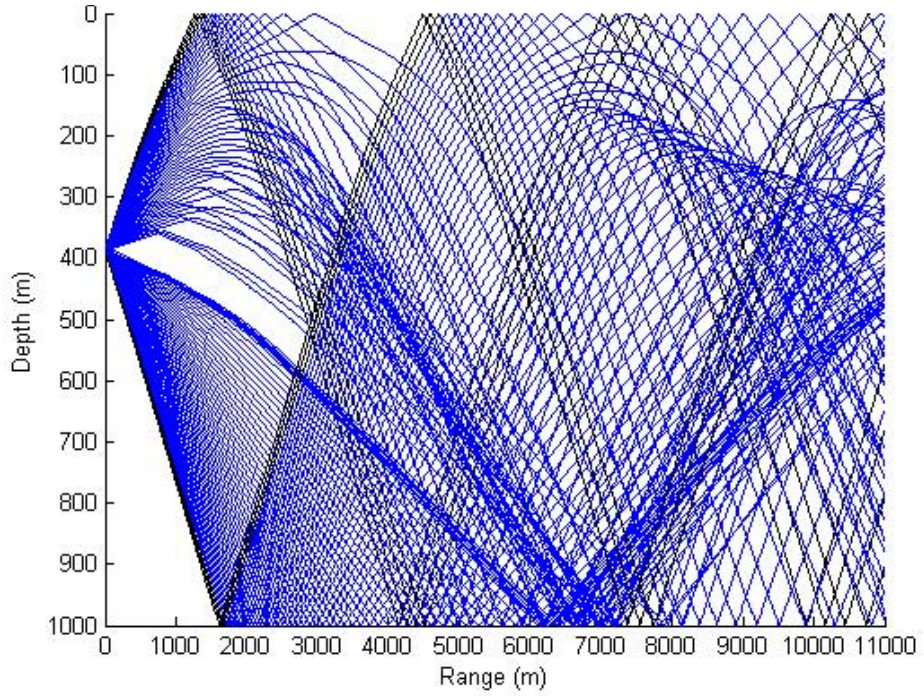

Figure 33. Ray Trace for source at 387 m (depth of an interface) in a staircase environment.

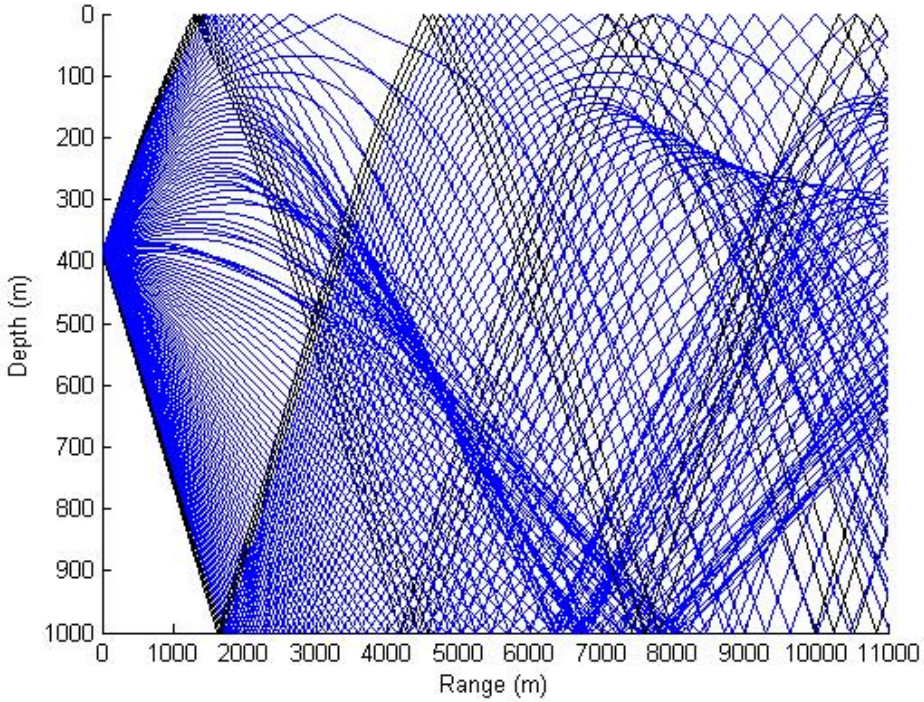

Figure 34. Ray trace for a source at 387 m in a smoothed profile.

b. Transmission Loss

Figures 35 to 40 displays transmission loss for both stepped and smooth profiles when the source is positioned at an interface, from 50 to 5000 Hz. As was evidenced in the ray trace of the stepped profile, a large shadow zone exists at this depth at all frequencies tested, which is not observed in the smooth profile (although at some frequencies there appears to be a small area of increased transmission loss above this in the smoothed profile). There is also an apparent weak concentration of signal in the area just below this shadow zone, reasons for this are unexplained.

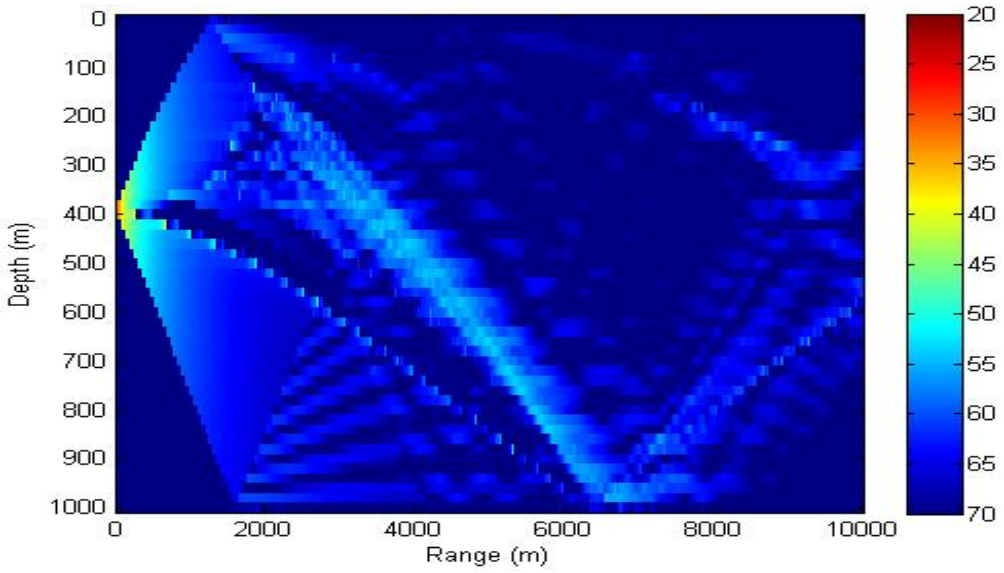

Figure 35. Coherent TL (dB/m) for stepped profile with source in interface at 50 Hz

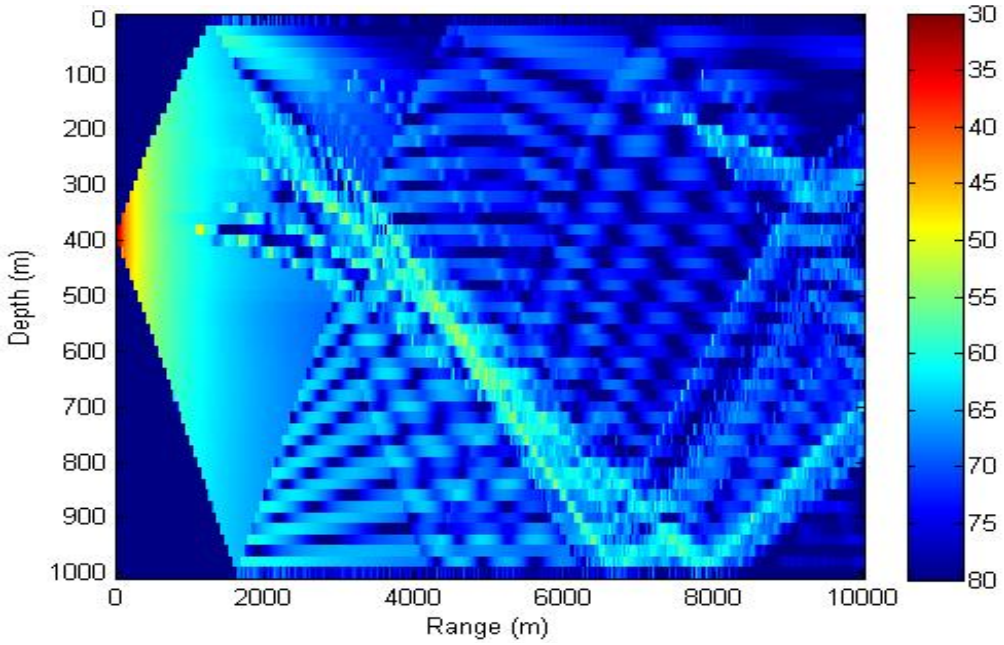

Figure 36. Coherent TL (dB/m) for smooth profile with 50 Hz source at 387 m.

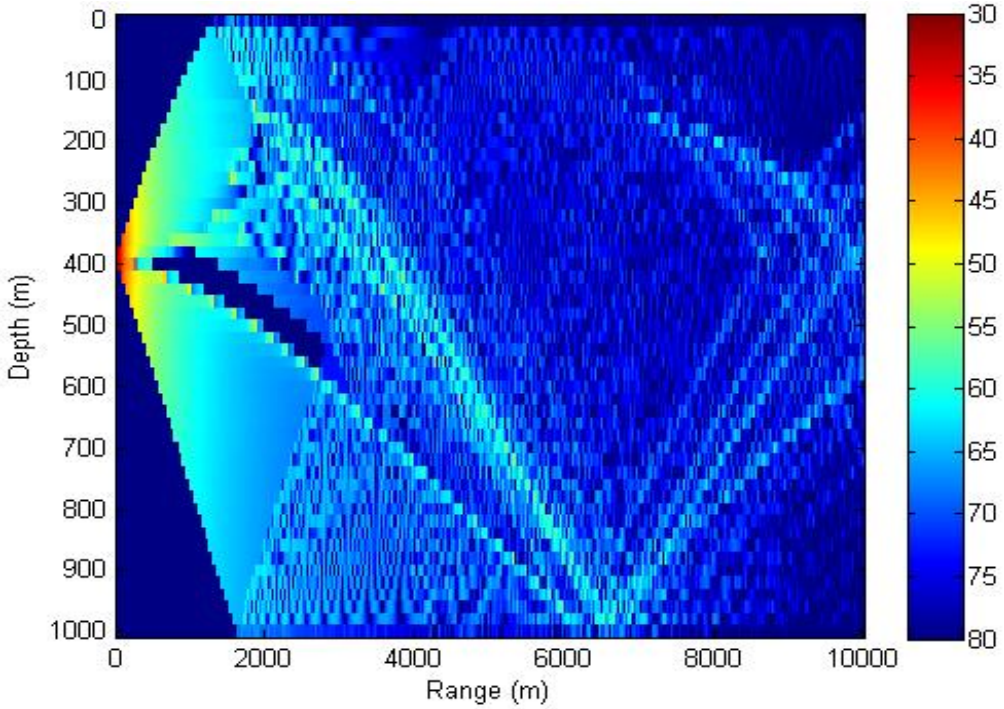

Figure 37. Coherent TL (dB/m) for stepped profile with source in interface at 2000 Hz.

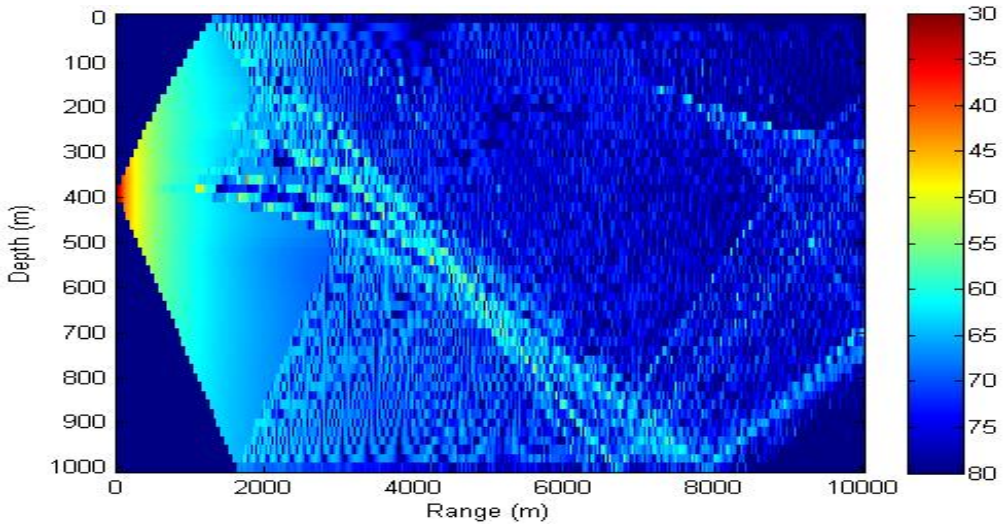

Figure 38. Coherent TL (dB/m) for smooth profile with 2000 Hz source at 387 m.

Increasing the frequency to 2000 Hz appears to have a pronounced effect on the shadow zone in the stepped profile.

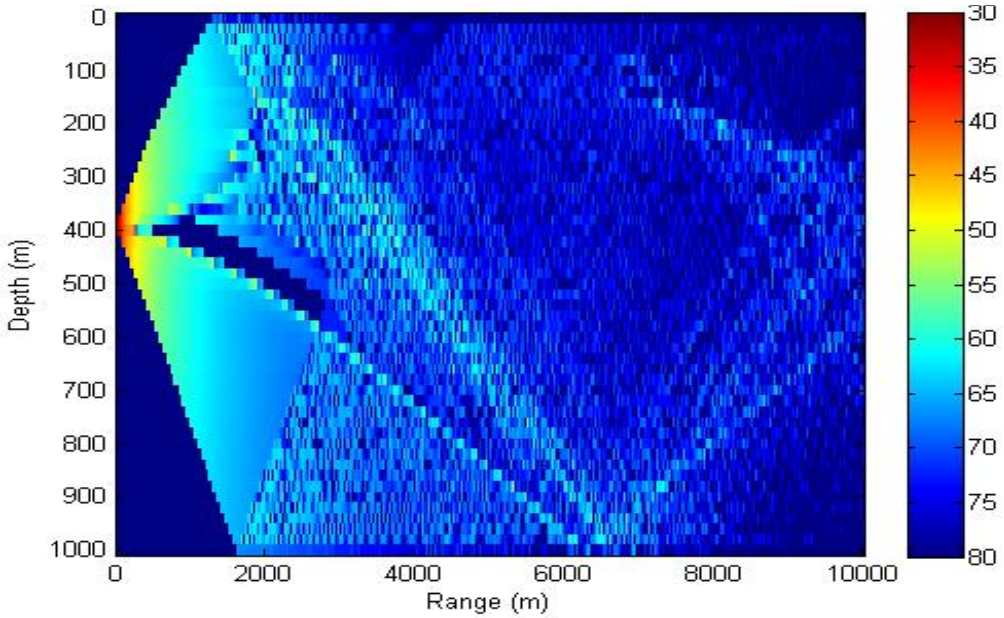

Figure 39. Coherent TL (dB/m) for stepped environment with source in interface at 5000 Hz.

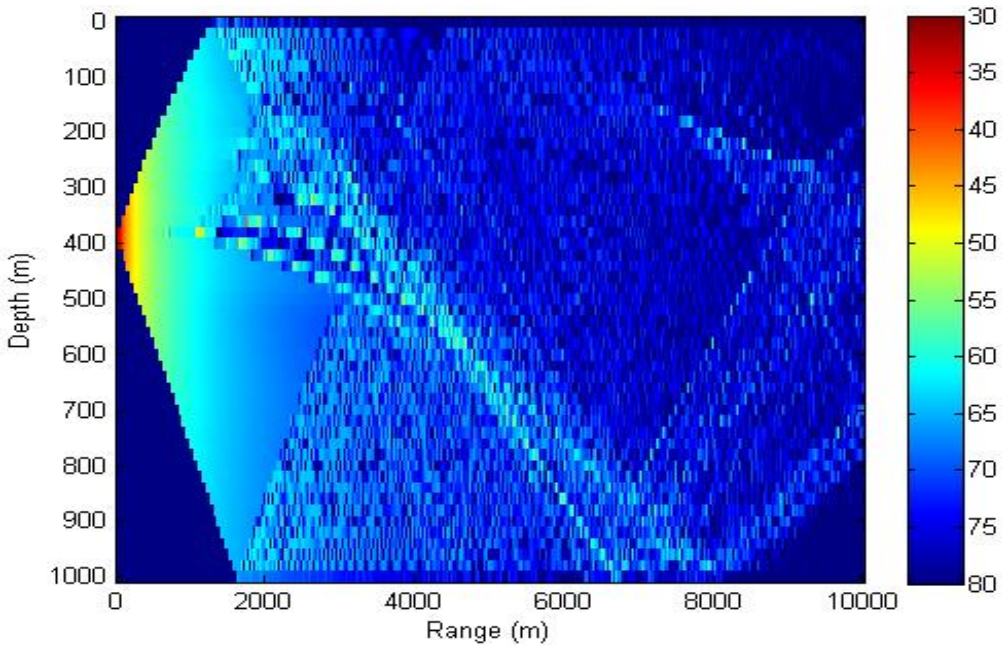

Figure 40. Coherent TL (dB/m) for 5000 Hz source in smooth profile at 387 m.

There is little obvious difference between 2000 Hz and 5000 Hz when the source is placed at the interface of a staircase

3. Source Depth 450 m

a. Ray Trace

In this scenario the source is positioned at a depth that corresponds to the center of a vertically mixed layer in the stepped profile. Unlike the previous example, in this case the low angle rays converge, causing a very obvious duct to occur at the source depth. In the smoothed profile, the ducting is not evident to the same extent, with no particular features of convergence or divergence appearing to stand out.

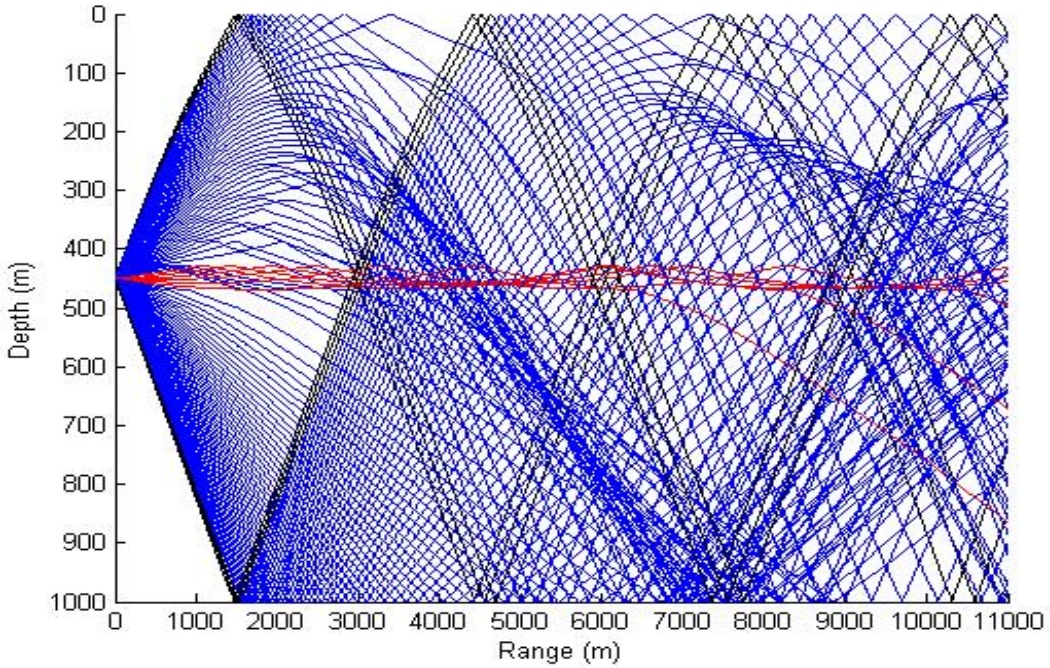

Figure 41. Ray trace with source at 450 m (center of vertically mixed layer) in a staircase environment.

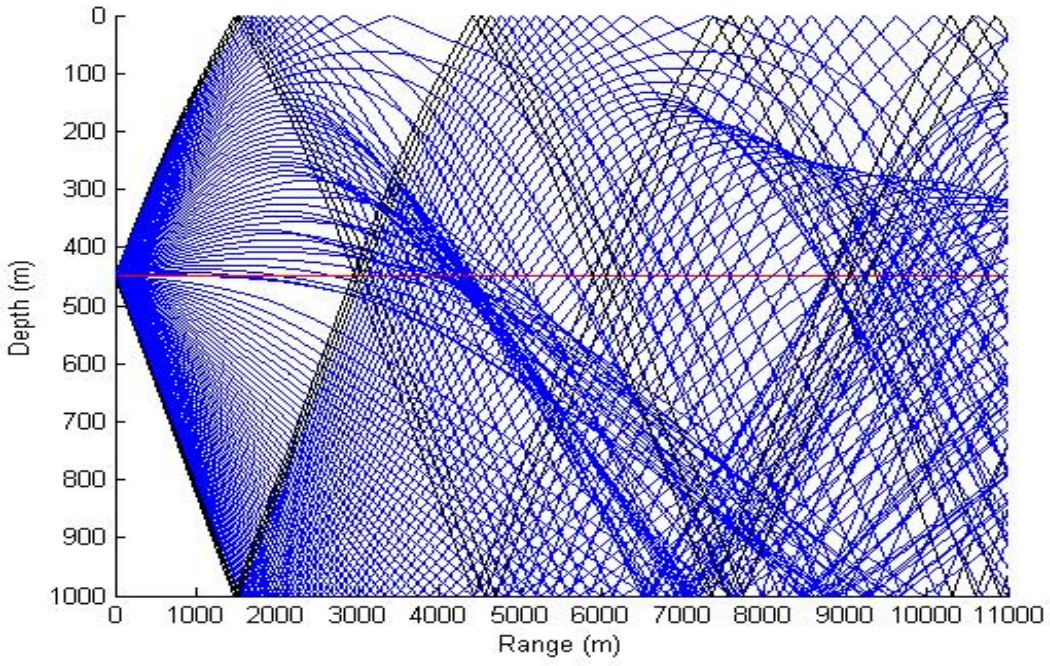

Figure 42. Ray trace with source depth 450 m in a smoothed profile.

b. Transmission Loss

The ducting that is observed in the ray trace using the stepped profile for a source at the center of the layer is also observed in all the TL plots. In the smoothed profile, all the plots are void of any ducting characteristics resultant from staircases. This demonstrates that if the source is placed within a layer of the staircase, that much higher horizontal acoustic ranges may be achieved than if there were no staircase present. Once again, examples are shown with lower and higher source frequencies. It is evident that an increase in frequency from 50 Hz to 2000 Hz results in higher propagation ranges within the duct, as a result of increased leakage at lower frequencies, as opposed to trapping of smaller wavelengths. However, there is not a significant difference between the ducted propagation of 2000 and 5000 Hz, and it is proposed that this is a result of the increased absorption loss at higher frequencies.

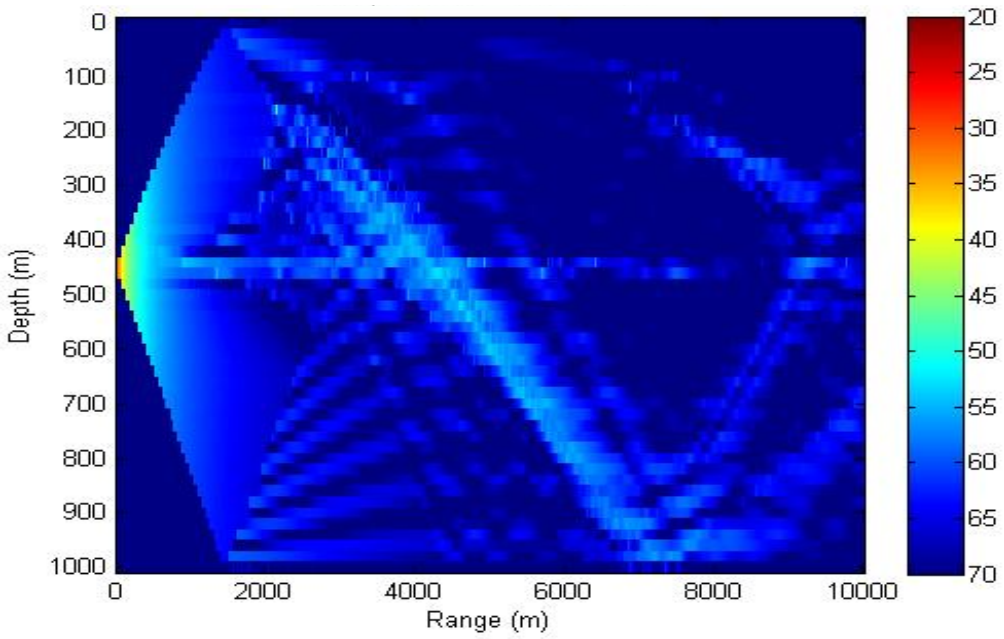

Figure 43. Coherent TL (dB/m) for stepped profile with 50 Hz source in layer.

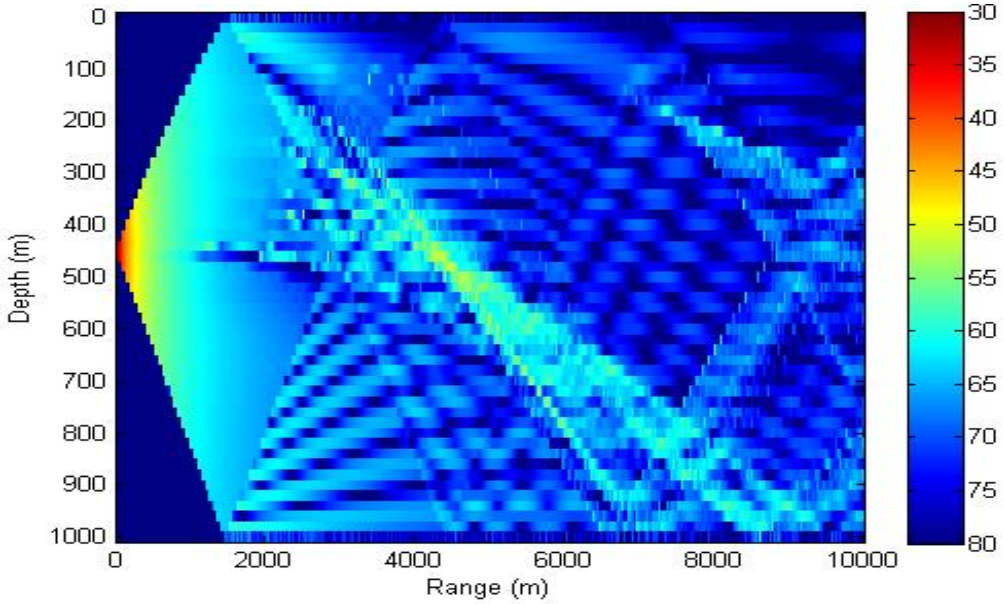

Figure 44. Coherent TL (dB/m) for 50Hz source at 450m in a smoothed environment.

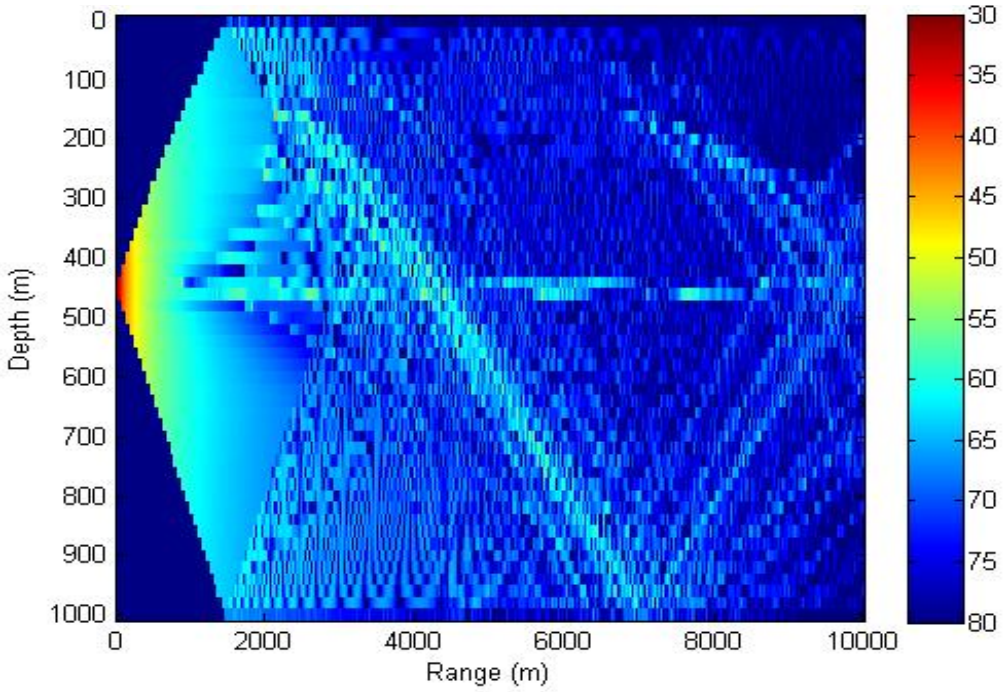

Figure 45. Coherent TL (dB/m) for stepped profile with 2000 Hz source in layer.

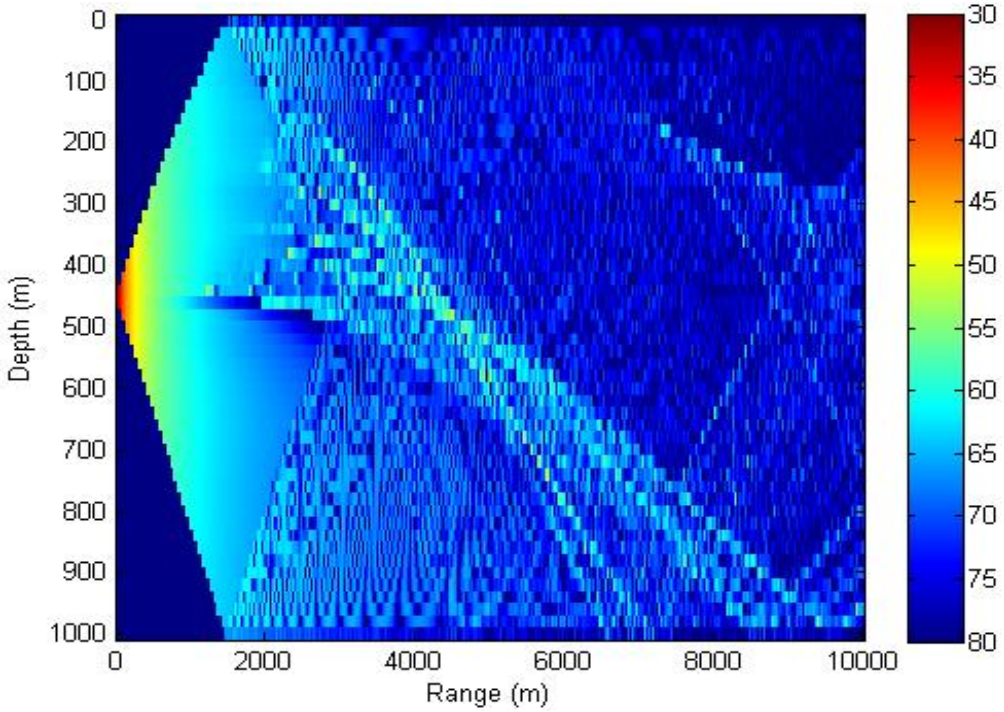

Figure 46. Coherent TL (dB/m) for 2000 Hz source at 450m in smoothed profile.

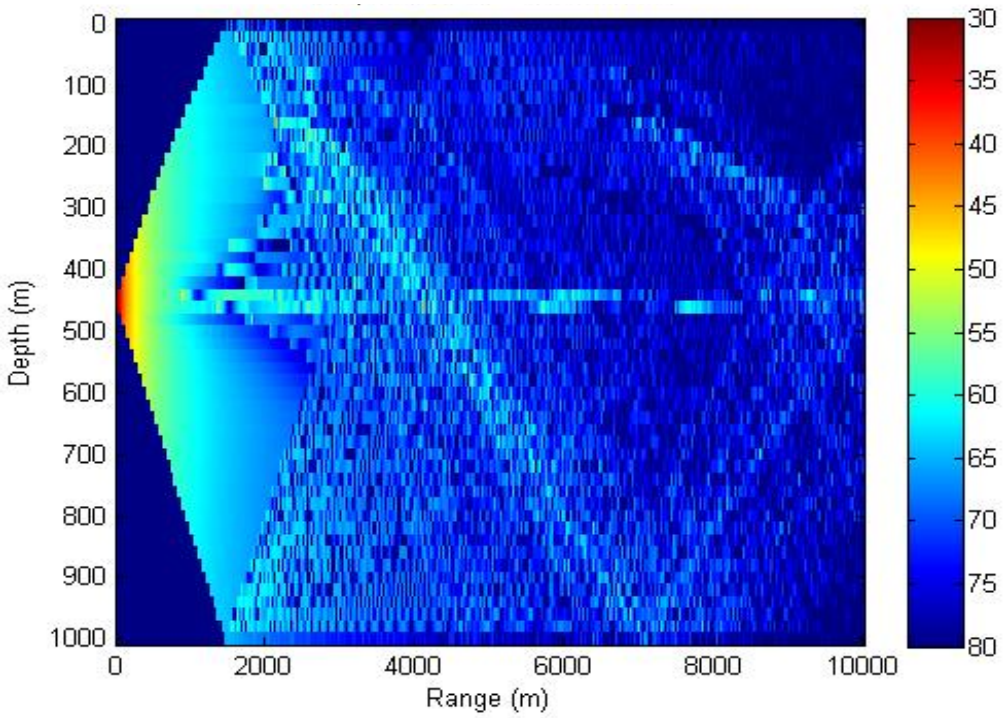

Figure 47. Coherent TL (dB/m) for 5000 Hz source in layer of stepped profile.

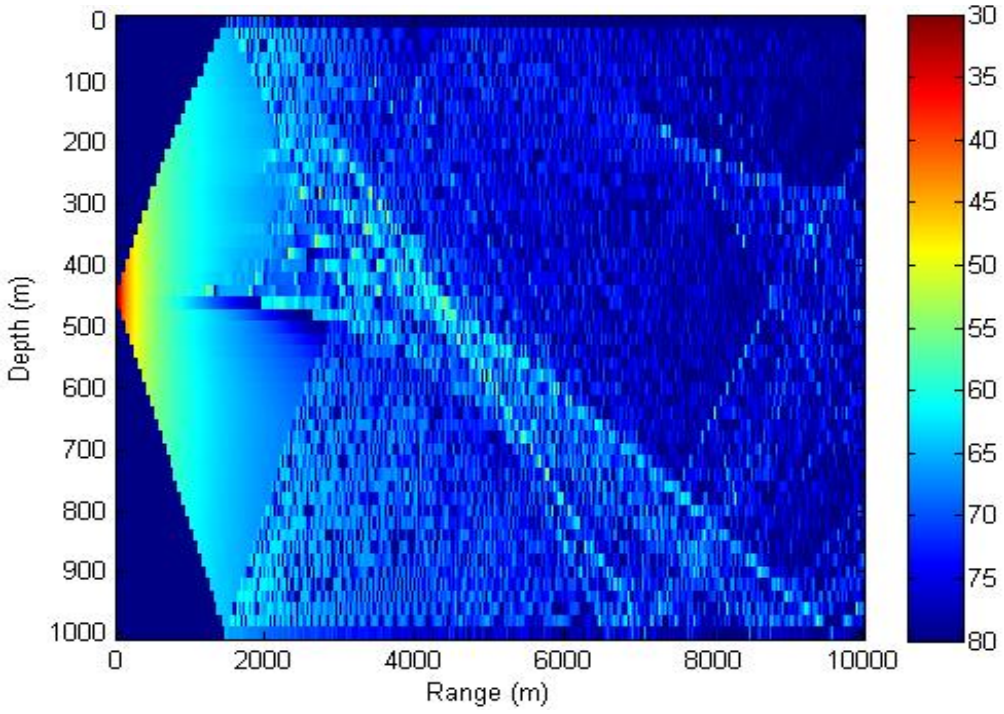

Figure 48. Coherent TL (dB/m) for 5000 Hz source at 450 m in smoothed profile.

4. Range-Dependent Source in Layer

a. Ray Trace

Following on from the investigation of a source placed in a staircase layer as opposed to a staircase interface, we investigate a range-dependent example of acoustic propagation in staircases. Figure 24 displayed a series of temperature profiles from the numerical model spaced every 10 km with lateral coherence over a range of 300 km. Nine adjacent profiles from this model were converted to SSP using the MATLAB acoustic toolbox and then compiled into a range-dependent input file compatible with Bellhop. Figure 50 shows the individual sound speed profiles, and Figure 51 displays an interpolated sound speed over the entire range showing the subtle shift in sound speed over range and depth as a result of small vertical shifts in the laterally coherent layers. The center of a 35 m vertical layer at a range of 0 m within the staircase region was identified at a depth of 785 m, and a ray trace was conducted with the source at this depth. Ducting is evident at this depth as can be seen by the red ray path in Figure 49. An interesting feature is a shift in the ducted rays at a range of approximately 60 km from the source. It is hypothesized that this is a result of a subtle shift in the depth of interfaces of connecting layers as range is increased away from the source. It is apparent from the ray trace that the duct shifts up or down to remain within the layer, as the layer thickness changes (interfaces shift up/down), over extended ranges.

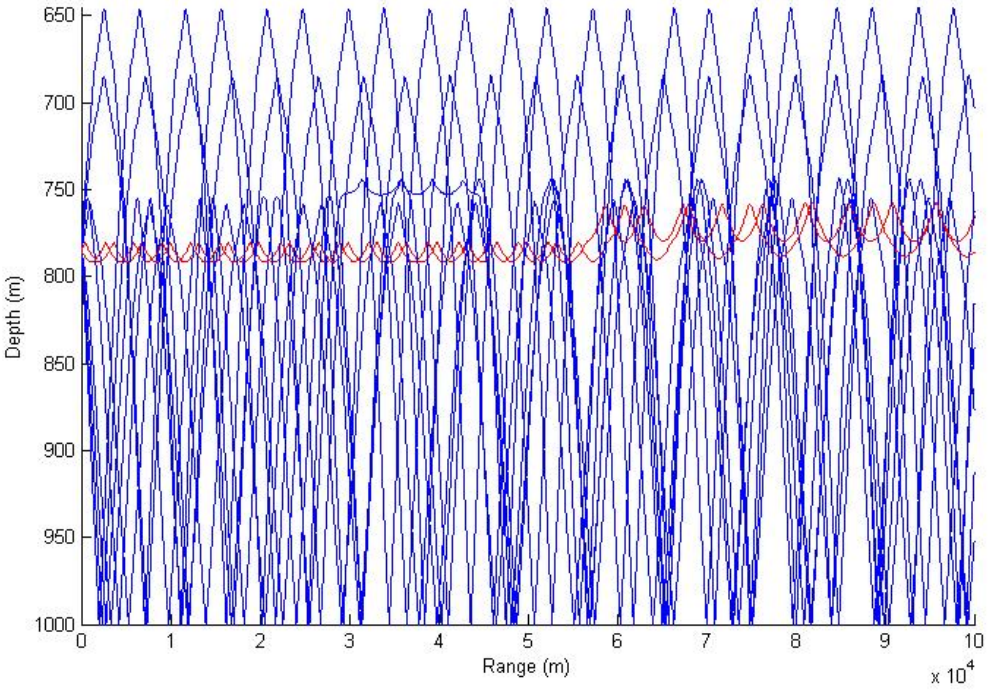

Figure 49. Ray trace for source at 785 m (source in layer), in a range dependent staircase environment.

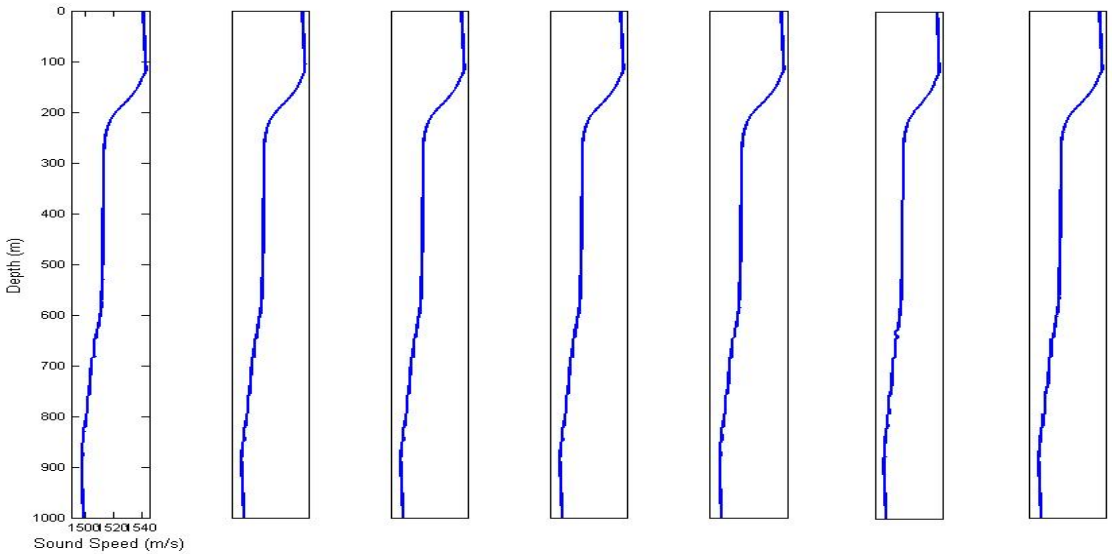

Figure 50. Range-dependent sound speed profiles at 10 km spacing.

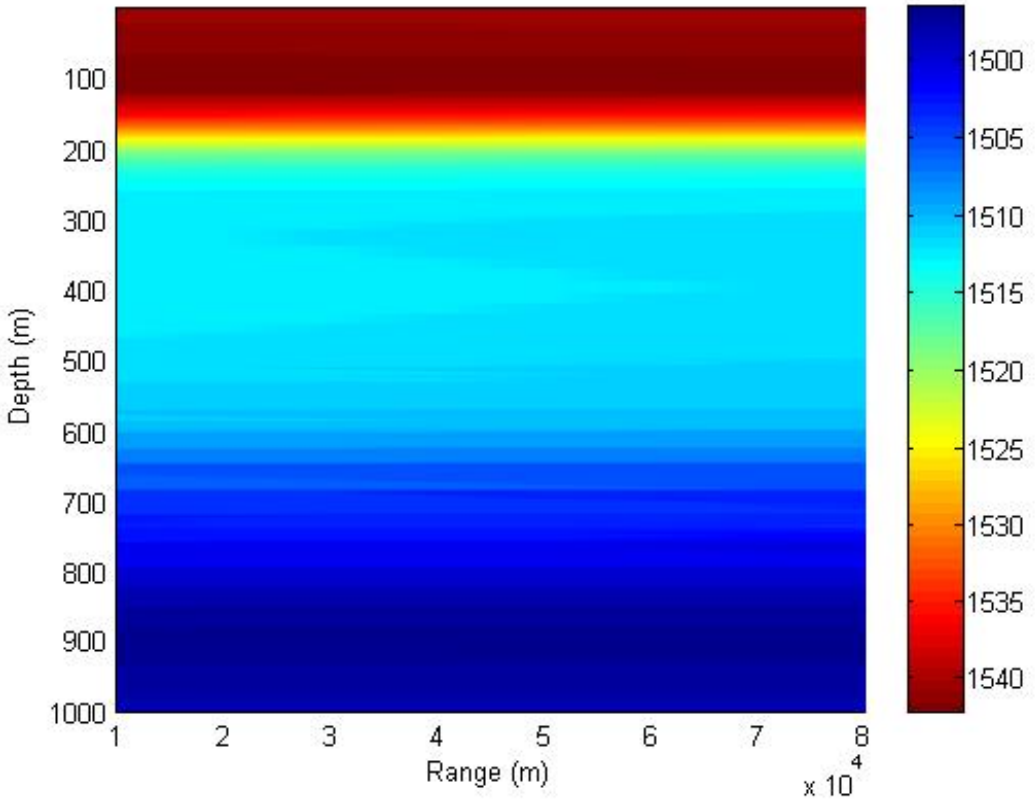

Figure 51. Sound speed (m/s) as a function of depth and range due to laterally coherent staircases.

b. Transmission Loss

Figure 52 to 55 displays transmission loss for the range-dependent case when the source is placed at 785 m within a prominent layer, over frequencies of 50 to 5000 Hz. A notable difference in analysis to earlier TL plots is that the TL is now being observed over a range of 100 km. Ducting is evident at the source depth in all cases with the exception of 50 Hz. In the 50 Hz scenario there is increased energy at this depth at short range, as a result of leakage. However, the larger wavelength means sound is not trapped in this layer. The best example of ducting occurs at 500 Hz, where there is very obvious trapping of the rays through the entire range, with significant energy

still remaining at 80 km from the source. The ducting is also obvious at 2000 Hz, but is largely diminished by 5000 Hz. It can be surmised that as the frequency of the source is increased the absorption at the higher frequencies quickly becomes a more dominant process. Therefore, in a range-dependent situation a low to medium frequency source of approximately 1000 Hz appears most effective in propagation of sound within a duct. It is proposed that this frequency is highly dependent on the thickness of the vertical layers also, as small layers are likely to only trap higher frequency rays.

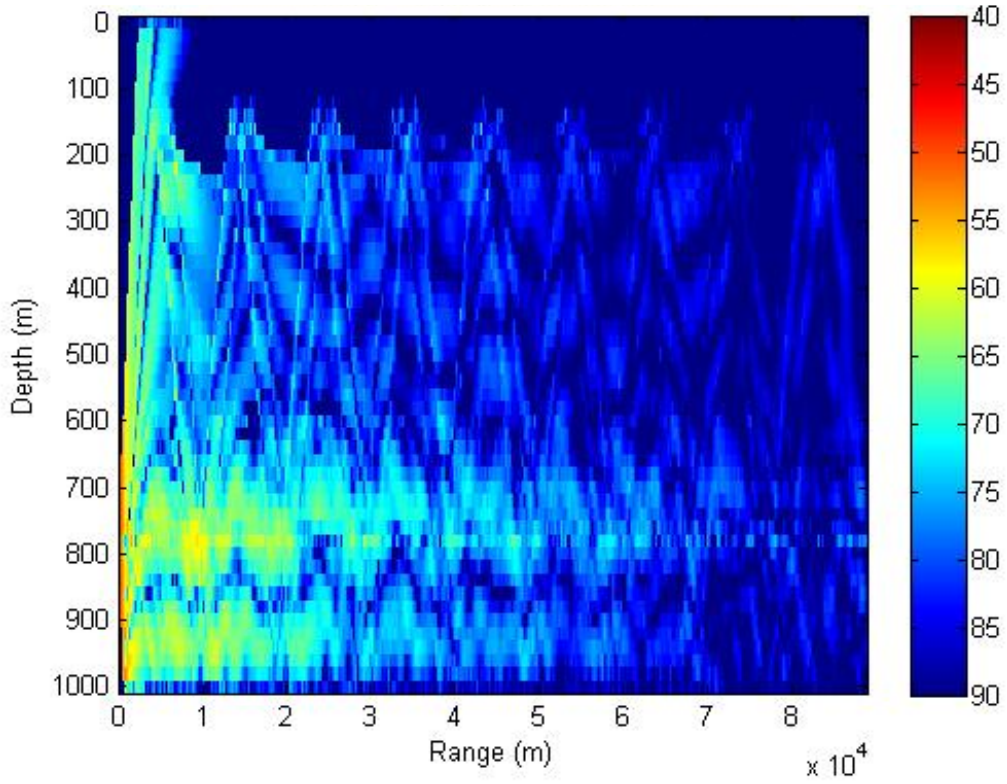

Figure 52. Coherent TL (dB/m) for 50 Hz source within layer.

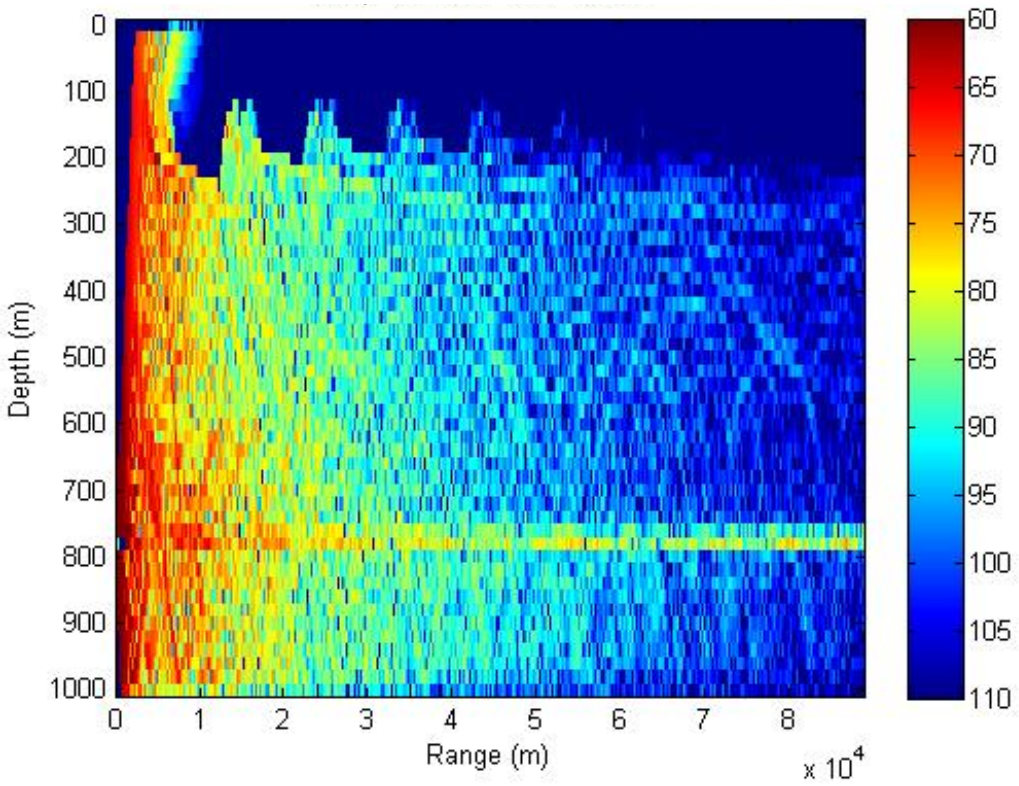

Figure 53. Coherent TL (dB/m) for 500 Hz within layer.

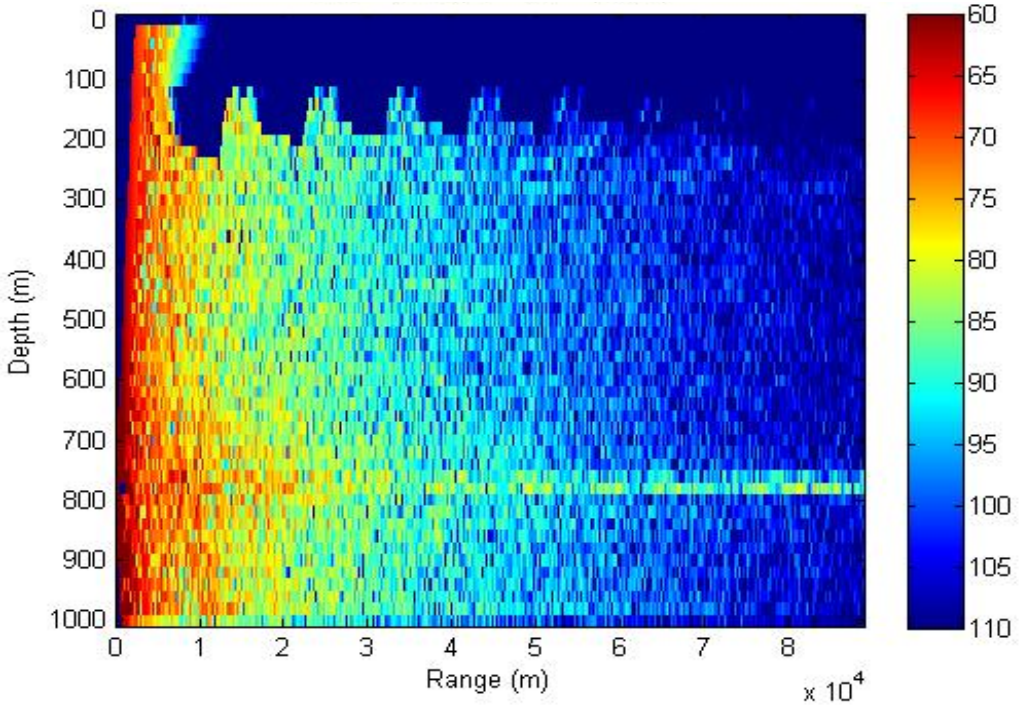

Figure 54. Coherent TL (dB/m) for 2000 Hz within layer.

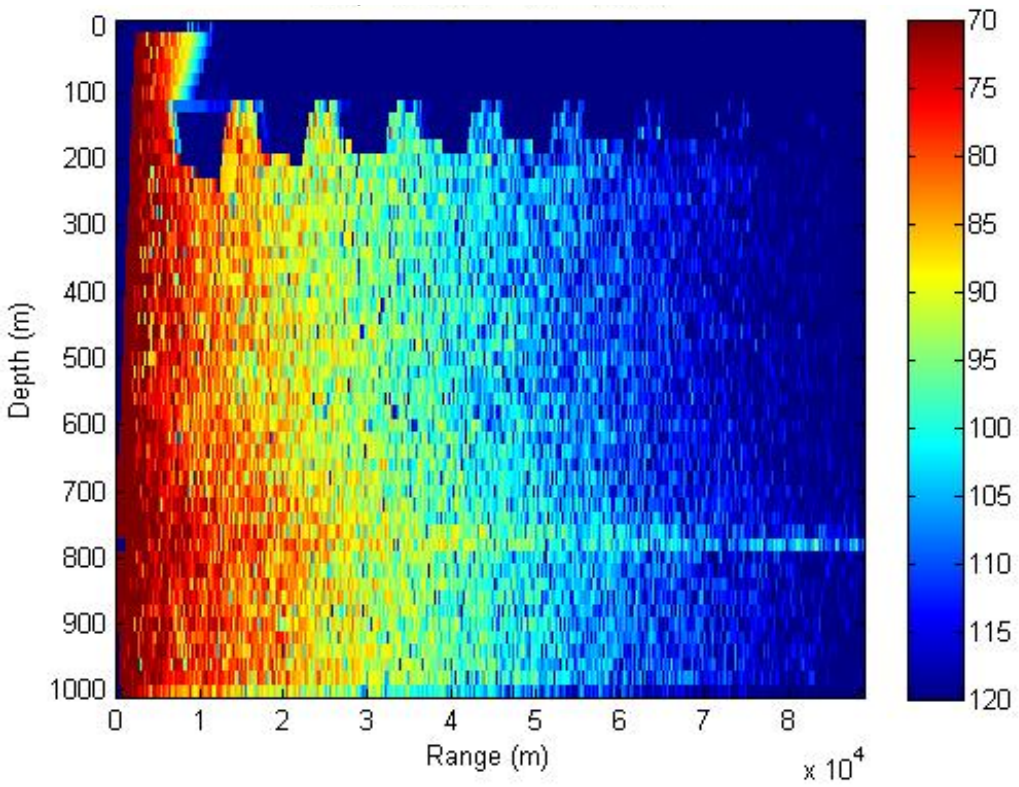

Figure 55. Coherent TL (dB/m) for 5000 Hz within a layer.

5. Range-Dependent Source in Interface

a. Ray Trace

Using the same range-dependent profiles from part 4, a source was placed at a depth of 750 m, which coincides with an interface. In the resultant ray trace from this there is no apparent ducting of the rays. Similarly to what was seen in the range-independent scenario previously discussed, there appears to be a divergence of the rays in a horizontal direction from the sound source as highlighted in the circle. Close to the sound source this may generate a shadow zone, however in the range dependent case this area is quickly flooded with energy from refracted and reflected rays.

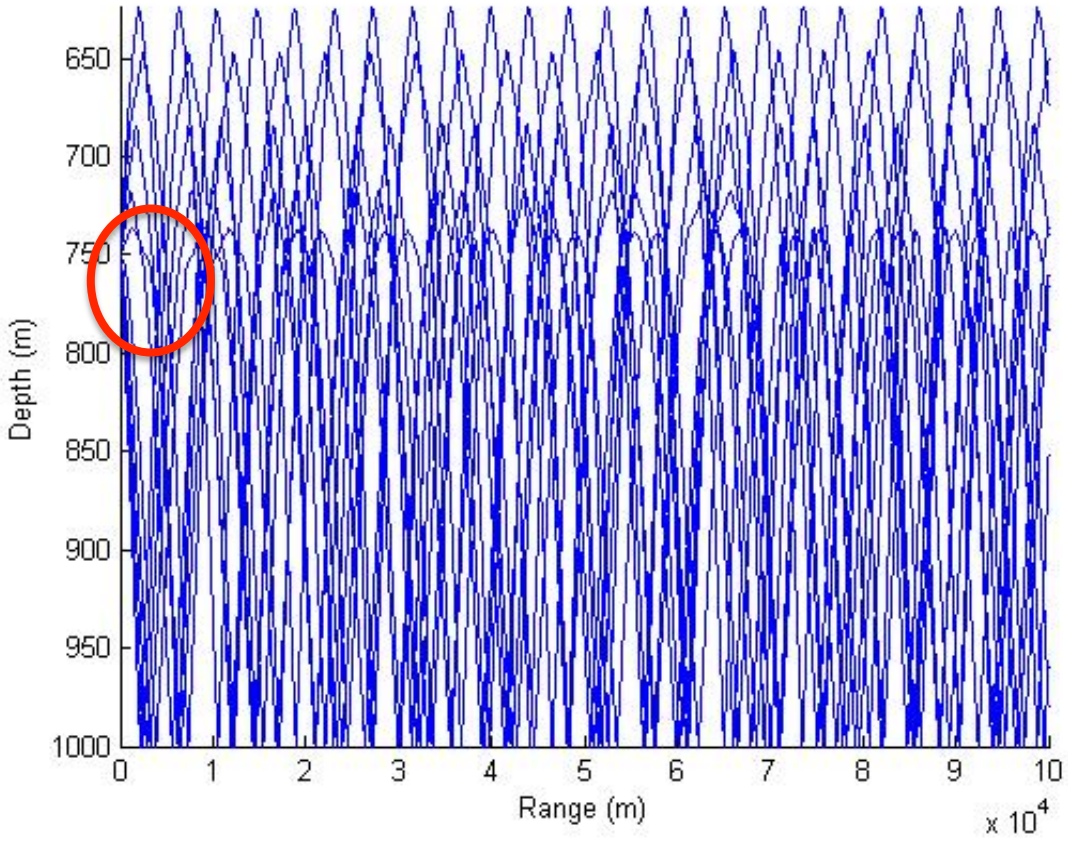

Figure 56. Ray trace for source at staircase interface for range-dependent profiles.

b. Transmission Loss

Transmission loss was again calculated from 50 to 5000 Hz for the source at the interface. It appears that some energy still manages to get trapped within the lower layer ducts, and there is faint evidence of this at a large range from the source of approximately 70 km, at 500 and 2000 Hz frequencies. This ducting effect is much less pronounced when the source is at the interface as opposed to the center of the layer.

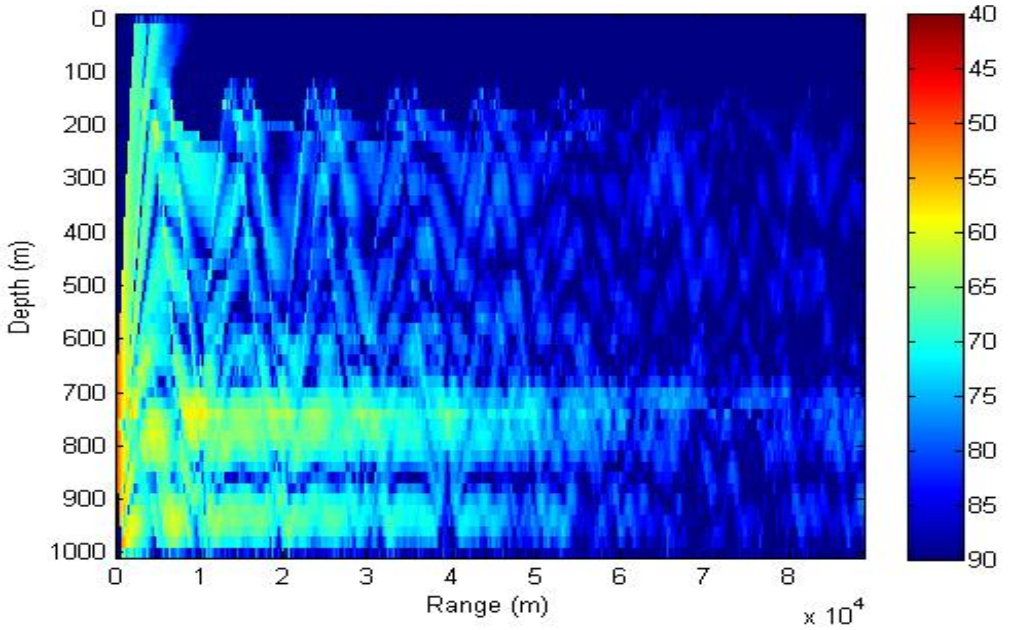

Figure 57. Coherent TL (dB/m) for 50 Hz source at interface.

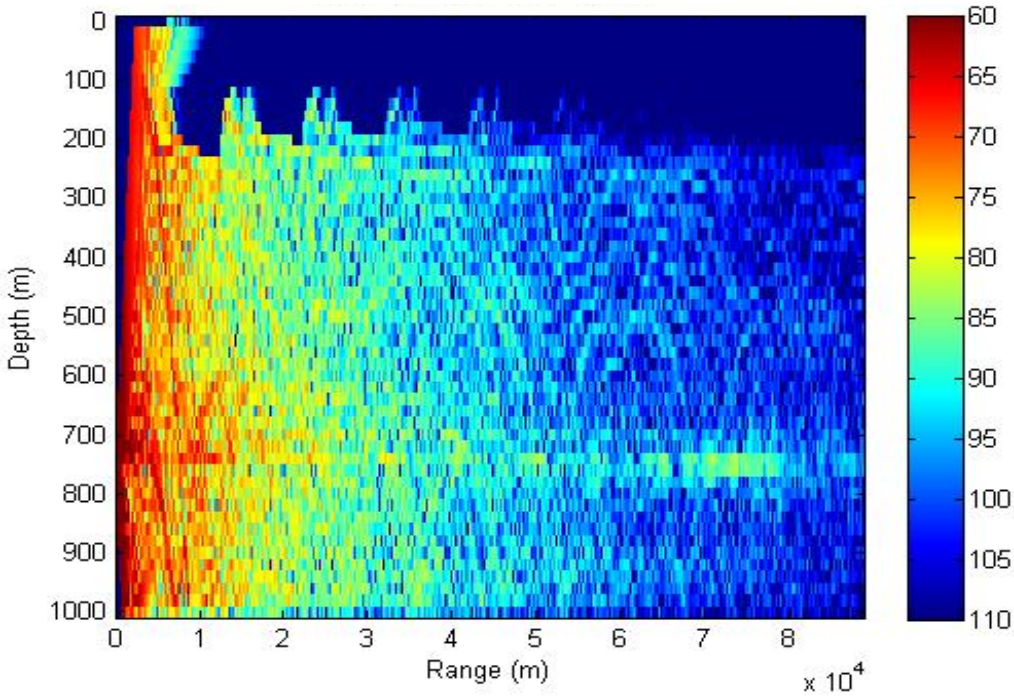

Figure 58. Coherent TL (dB/m) for 500 Hz source at interface.

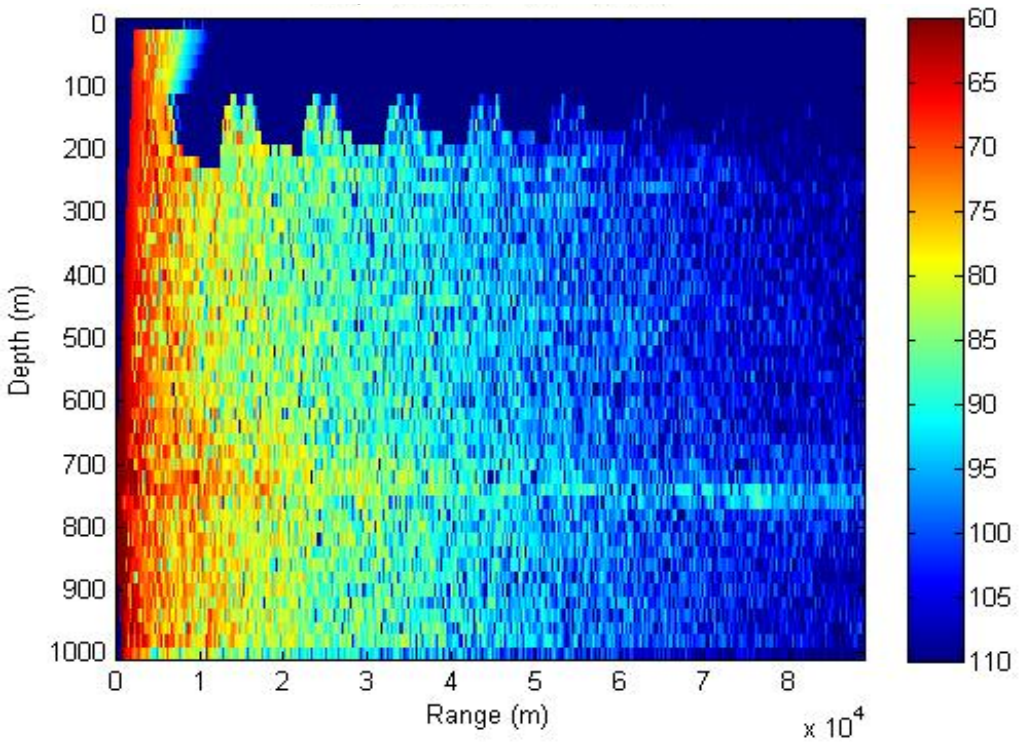

Figure 59. Coherent TL (dB/m) for 2000 Hz source at interface.

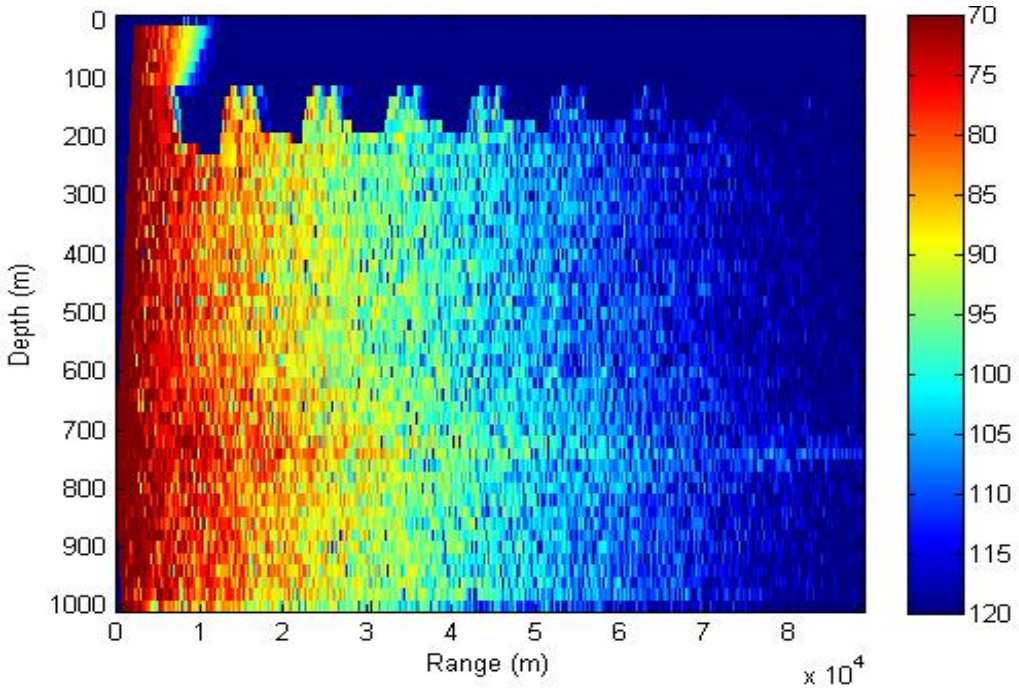

Figure 60. Coherent TL (dB/m) for 5000 Hz source at interface depth.

THIS PAGE INTENTIONALLY LEFT BLANK

V. CONCLUSIONS

Thermohaline staircases are a significant feature of ocean mixing, and this study has aimed to explore staircase evolution in three dimensions as a result of salt fingering, through numerical simulation.

A large task was undertaken in attempting to simulate three dimensional staircases over an entire ocean basin. To the authors' best knowledge this is the first basin-scale simulation that exhibits spontaneous layering. A promising result has been the modeling of laterally coherent staircases over several hundreds of kilometers in the ocean. This provides an interesting area of further research, particularly with the alignment of layer interfaces with background isotherms. While this was not achieved in this thesis, it is proposed that Wall's hypothesis of a correlated layer slope with thermohaline will hold true, and with more computing hours and time, it is believed that a high resolution grid would make this an achievable task for researchers in the future.

This study aimed to parameterize turbulent diffusivity through the process of trial and elimination in order to closely simulate the thermohaline staircases seen in the C-SALT observation area. Through this process, the turbulent diffusivity was indirectly estimated at 2.5 x 10^{-6} m^2/s.

A comparison between the gamma-effect variation in the flux ratio with the density ratio confirmed a very distinct link between the flux ratio, the density ratio, and staircase formation. This lends further support to the flux ratio model of Radko and Smith (2012).

The numerical simulation of merging events indicates the prevalence of instability that leads to the 'B type merger' as discussed in Radko (2007), and this simulation clearly supports the theory that development of thermohaline staircases by salt fingers is a direct result of strong interfaces growing at the expense of weaker ones which ultimately erode.

The acoustic propagation modeling through the staircase of both the C-SALT profiles and the numerical model indicate that thermohaline staircases have a very pronounced effect on sound propagation, which is accentuated with position placement of the sound source within the staircase. The ducting that occurs when a source is placed centrally within a layer of a staircase is a significant feature, and the increased range of the duct with lateral coherence of staircases is an extremely important facet to be considered in acoustic modeling. Understanding where staircase regions of lateral coherence occur, coupled with knowledge of interface and layer depths within this region can be of critical importance for tactical employment of submarines, gliders, variable depth sonars, torpedo homing, and other underwater vehicles within this region. This information, combined with an awareness of the impact of differing source frequencies on the ducting, can result in a significant exploitation of the environment for tactical purposes.

LIST OF REFERENCES

Adcroft, A., and Coauthors, cited 2012: MITGCM User Manual. [Available online at http://mitgcm.org/public/docs.html]

Chin-Bing, S.A., D.B. King, and J.D. Boyd, 1994: The Effects of Ocean Environmental Variability on Underwater Acoustic Propogation Forecasting. *Oceanography and Acoustics Prediction and Propogation Models*, A.R. Robinson and D. Lee, Eds., American Institute of Physics Press, 7-49.

Gent, P.R, and J.C. McWilliams, 1990: Isopycnal mising in ocean circulation models, *J. Phys. Oceanogr.*, **20**, 150-155.

Hamilton, E.L., 1980: Geoacoustic modeling of the sea floor. *J. Acoust. Soc. Am.*, **68**, 1313-1340.

Huppert, H.E., 1971: On the Stability of a series of Double-Diffusive Layers, *Deep-Sea Res.*, **18**, 1005-1021.

Kelley, D.E., 1990: Fluxes Through Diffusive Staircases: A New Formulation, *J. Geophys. Res.*, **95**, 3365-3371.

Large, W.G., J.C. McWilliams, and S.C. Doney, 1994: Oceanic vertical mixing: A review and a model with a nonlocal boundary layer parameterization. *Rev. Geophys.*, **32**, 363-403.

Large, W.G., G. Danabasoglu, S.D. Doney, and J.C. McWilliams, 1997: Sensitivity to surface forcing and boundary layer mixing in a global ocean model: Annual-mean climatology, *J. Phys. Oceanogr.*, **27**, 2418-2447.

Merryfield, W.J., 2000: Origin of thermohaline staircases. *J. Phys. Oceanogr.*, **30**, 1046-1068.

National Oceanographic & Atmospheric Administration, cited 2012: NODC_WOA98. [Available online at http://www.esrl.noaa.gov/psd/]

Packanowski, R.C., and Griffies, S.M., cited 2012: MOM 3.0 Manual Draft Manual 2000. [Available online at http://gfdl.noaa.gov/cms-fliesystem-action/model_development/ocean/mom3_manual.pdf]

Porter, M.B., cited 2012: The Bellhop Manual and User's Guide: Preliminary Draft. [Available online at http://oalib.hlsresearch.com/Rays/HLS-2010-1.pdf]

Radko, T., 2003: A mechanism for layer formation in a double-diffusive fluid. *J. Fluid Mech.*, **497**, 365–380

Radko, T., 2005: What determines the thickness of layers in a thermohaline staircase? *J. Fluid Mech.*, **523**, 79–98.

Radko, T., 2007: Mechanics of merging events for a series of layers in a stratified turbulent fluid. *J. Fluid Mech.*, **577**, 251–273.

Radko, T. and D.P. Smith, 2012: Equilibrium transport in double-diffusive convection, *J. Fluid Mech.*, **692**, 5–27.

Redi, M.H., 1982: Oceanic Isopycnal mixing by coordinate rotation. *J. Phys. Oceanogr.*, **12**, 1154–1158

Rodriguez, O.C., cited 2012: General description of the Bellhop ray tracing program.[Available online at http://www.siplab.fct.ualg.pt/models/bellhop/manual.pdf]

Ruddick, B., and O. Kerr, 2003: Oceanic thermohaline intrusions: theory. *Progress in Oceanogr.*, **56**, 483–497.

Schmitt, R.W., 1987: The Caribbean Sheets and Layers Transects (C-SALT) Program. *Eos*, **68**, 57–60.

Schmitt, R.W., H. Perkins, J.D. Boyd, and M.C. Stalcup, 1987: C-SALT: an investigation of the thermohaline staircase in the western tropical North Atlantic. *Deep-Sea Research*, **34**, 1655–1665.

Schmitt, R.W., 1988: Mixing in a Thermohaline Staircase, *Small-Scale Turbulence and Mixing in the Ocean*, J.C.J. Nihoul and B.M. Jamart, Eds., Elsevier, 438–452.

Schmitt, R.W., 1995: The Ocean's Salt Fingers, *Scientific American,* **272**, 70–75.

Schmitt, R.W., J.R.Ledwell, E.T. Montgomery, K.L. Polzin, and J.M. Toole, 2005: Enhanced Diapycnal Mixing by Salt Fingers in the Thermocline of the Tropical Atlantic, *Science,* **308**, 685–688.

Stern, M.E., 1960: The 'salt fountain' and thermohaline convection. *Tellus.* **12**, 172–175.

Stern, M.E. and J.S. Turner, 1969: Salt fingers and convecting layers. *Deep-Sea Res.,* **16**, 497–511.

Stommel, H., A.B Arons and D. Blanchard, 1956: An oceanographical curiosity: the perpetual salt fountain. *Deep-Sea Res.,* **3**, 152–153.

Timmermans, M.L., J. Toole, R. Krishfield, and P.Winsor, 2008: Ice-Tethered Profiler observations of the double-diffusive staircase in the Canada Basin thermocline. *J. Geophys. Res.,* **113**, doi:10.1029/2008JC004829

Turner, J.S., 1973: *Buoyancy Effects in Fluids*. Cambridge University Press, 367 pp.

Wall, S.E., 2007: Structure and Evolution of Thermohaline Staircases in Tropical North Atlantic, Dept. of Oceanography, Naval Postgraduate School, 87 pp.

Wilson, A.L., 2007: Structure and Dynamics of the Thermohaline Staircases in the Beaufort Gyre, Dept. of Oceanography, Naval Postgraduate School, 59 pp.

THIS PAGE INTENTIONALLY LEFT BLANK

INITIAL DISTRIBUTION LIST

1. Defense Technical Information Center
   Ft. Belvoir, Virginia

2. Dudley Knox Library
   Naval Postgraduate School
   Monterey, California

3. Dr. Peter Chu
   Naval Postgraduate School
   Monterey, California

4. Dr. Timour Radko
   Naval Postgraduate School
   Monterey, California

5. Dr. Jason Flanagan
   Naval Postgraduate School
   Monterey, California

6. John Joseph
   Naval Postgraduate School
   Monterey, California

7. Directorate of Oceanography and Meteorology
   Wollongong, New South Wales, Australia

8. Physical Sciences Division: Data Management
   NOAA/ESRL/PSD
   Boulder, Colorado